

# Fabrication a novel ethylenediamine sulfonamide polymer resin and graphene-modified carbon paste electrodes for simultaneous determination of anti-HBV drugs entecavir and tenofovir in dosage form by differential pulse voltammetry

Adel ASFOOR<sup>1,2</sup> , Zeynep AYDOĞMUŞ<sup>1\*</sup> , Bahire Filiz SENKAL<sup>3</sup> 

<sup>1</sup> Department of Analytical Chemistry, Faculty of Pharmacy, Istanbul University, Beyazıt, 34116 Istanbul, Turkey.

<sup>2</sup> Istanbul University, Institute of Graduate Studies in Health Sciences, Beyazıt, 34116 Istanbul, Turkey.

<sup>3</sup> Department of Chemistry, Faculty of Science and Letters, Istanbul Technical University 2, Maslak, 34469 Istanbul, Turkey.

\* Corresponding Author. E-mail: [aydogmus@istanbul.edu.tr](mailto:aydogmus@istanbul.edu.tr) (Z.A.); Tel. +90-533-572 62 26.

Received: 02 June 2023 / Revised: 06 August 2023 / Accepted: 07 August 2023

**ABSTRACT:** The combination of entecavir (ETV) and tenofovir (TEV), nucleos(t)ide analogs (NUCs), is advised as first-line treatment for people suffering from multidrug-resistant hepatitis B due to their favorable safety profile, low side-effect rate, and high genetic barrier. This study reports the fabrication of a novel cross-linked ethylenediamine sulfonamide polymer resin (EDASP) and graphene (Gr)-modified carbon paste electrodes (CPE) for the simultaneous determination of the anti-HBV drugs ETV and TEV in bulk and dosage form by differential pulse voltammetry (DPV). The electrodes were specified through cyclic voltammetry, Fourier transform infrared (FTIR), scanning electron microscopy (SEM), and the analytical parameters were optimized. The findings indicate that both drugs displayed clear oxidation peaks on the Gr-CPE and EDASP-CPE electrodes at pH 4.5 and 4.0, respectively, in the Britton-Robinson buffer. The linear dynamic range of ETV and TEV was determined between 1 μM and 250 μM on both working electrodes by DPV. The limit of detection (LOD) and limit of quantification (LOQ) for ETV were 0.2 μM and 0.6 μM, respectively, on Gr-CPE. The LOD and LOQ for TEV were 0.2 μM and 0.7 μM, respectively. The novel EDASP-CPE exhibited improved sensitivity with LOD and LOQ for ETV of 0.2 μM and 0.5 μM, respectively. The LOD and LOQ for TEV on EDASP CPE were 0.2 μM and 0.7 μM, respectively. The proposed method was successfully applied to the simultaneous determination of ETV and TEV in a commercial tablet dosage form, exhibiting good accuracy and precision. The results highlight the potential of the novel cross-linked ethylenediamine sulfonamide polymer resin-modified carbon paste electrode for the simultaneous determination of anti-HBV drugs in dosage form by differential pulse voltammetry.

**KEYWORDS:** Tenofovir, entecavir, ethylenediamine sulfonamide polymer resin, graphene, modified carbon paste electrode, voltammetry, pharmaceutical preparation.

## 1. INTRODUCTION

Hepatitis B virus (HBV) is a significant global health concern, with a considerable number of individuals affected worldwide, including those with chronic hepatitis B. HBV is a leading cause of mortality worldwide, contributing to a significant number of deaths every year, including those caused by chronic cirrhosis, hepatitis, and hepatocellular carcinoma. The annual death toll from HBV ranges from 500,000 to 1.2 million, with 320,000 deaths specifically caused by hepatocellular carcinoma [1]. Chronic HBV infection is frequently associated with chronic hepatitis C (HCV), which poses a significant threat to public health worldwide [2]. Individuals with both infections are at higher risk of developing severe liver disorders, such as cirrhosis and hepatocellular carcinoma [3]. The therapeutic regimens for anti-HBV and anti-HCV treatments, or both, vary depending on the status of the viral infections [4, 5]. Current guidelines recommend using a combination of Tenofovir disoproxil fumarate (TEV) and Entecavir (ETV) as first-line therapy for chronic hepatitis B (CHB) [6-10]. Both ETV and TEV have several advantages in common when it comes to treating CHB, such as high

**How to cite this article:** Aspoor A, Aydoğmuş Z, Senkal BF. Fabrication a novel ethylenediamine sulfonamide polymer resin and graphene-modified carbon paste electrodes for simultaneous determination of anti-HBV drugs entecavir and tenofovir in dosage form by differential pulse voltammetry. *J ResPharm.* 2024; 28(3): 579-602.

efficacy against viruses, good tolerability, and providing a robust barrier against resistance. Additionally, the development of resistance to these medications is challenging.

ETV is an antiviral drug known chemically as 2-amino-9-[(1S, 3R, 4S)-4-hydroxy-3-(hydroxymethyl)-2-methylidenecyclopentyl]-6,9-dihydro-1H-purin-6-one hydrate [11]. It is a carbocyclic 2'-deoxyguanosine nucleoside derivative that inhibits DNA replication and reverses transcription. It is prescribed to people with chronic hepatitis B and HIV infection [12]. ETV is currently the most effective anti-HBV drug [6, 13]. Various analytical methods have been described in the literature for measuring ETV in both drug formulations and biological fluids, including spectrophotometry (UV and FT-IR) [14-16], liquid chromatography [17, 18], liquid chromatography-tandem mass spectrometry [19, 20], ultra-high performance liquid chromatography-tandem mass spectrometry (UHPLC-MS/MS) [21, 22], and electrochemical methods [1, 23-25].

Tenofovir (TEV) is a nucleoside analogue of adenosine 5'-monophosphate, 1-(6-aminopurin-9-yl)propan-2-ylloxymethylphosphonic acid [26]. It is a reverse transcriptase inhibitor that is used to treat Human Immunodeficiency Virus (HIV) infections by inhibiting reverse transcriptase, an enzyme that is crucial for the replication of the virus [27, 28]. It also has significant anti-HBV potency and can treat HBV infections. It exhibits high efficacy against both viruses and is frequently used in combination with other antiretroviral medicines or as a monotherapy. It is prepared as a prodrug in pharmaceutical form as tenofovir disoproxil fumarate and tenofovir alafenamide fumarate.

Various analytical techniques have been established for determining the concentration of TEV in pharmaceuticals, human plasma, and other biological specimens. These techniques include spectrophotometry [29-31], mass spectrometry [32], reverse-phase high-performance liquid chromatography with diode array detection (RP-HPLC-DAD) [33, 34], liquid chromatography-mass spectrometry (LC-MS) [35], liquid chromatography-tandem mass spectrometry (LC-MS/MS) [36], and various electrochemical methods [37-45]. However, there are limited techniques available for the simultaneous quantification of both Tenofovir and Entecavir [46, 47], and none of them include simultaneous voltammetric measurements. Furthermore, most of these techniques require a lengthy process, expensive, time-consuming solid-phase extractions (SPE), salting-out processes [22, 48], and excessive use of expensive solvents, resulting in environmental pollution. During the treatment of HIV and Hepatitis B, patients often experience dystrophic changes and lesion formation in their body, as well as renal and skeletal system side effects due to the use of immunosuppressive and multiple drugs. Therefore, there is still a need for simple, rapid, selective, and sensitive methods for the determination of both drugs that could help in monitoring and adjusting the dose of the drug in the patient's treatment.

Electrochemical methods, particularly voltammetry, chemical electrodes, and biosensors, are becoming increasingly popular in the detection of organic compounds such as medications and similar compounds in pharmaceuticals and biological matrices. This is due to their advantages, including high specificity, sensitivity, ease of use, negligible cost, quick response time, and short analysis time [49]. The increasing interest in voltammetry is closely related to the development of electrode materials and instrument measurement modes. Various chemical and biological micro/nanomaterials have been synthesized and utilized as electrode materials in voltammetric methods, leading to improved sensitivity, selectivity, and stability of the sensors. Differential pulse voltammetry (DPV) is one of the voltammetric methods that can detect various substances with very high sensitivity. In this method, periodic pulses are applied to the working electrode during a linear scan, and the difference between the current just before the pulse and the current toward the end of the pulse is measured, resulting in a high faradaic current and a low capacitive current. In addition to voltammetric techniques, amperometric and potentiometric electrochemical methods are also frequently used in the quantification of substances in various matrices.

Carbon paste electrodes (CPEs) are commonly used in electroanalytical methods, and their surfaces can be modified with various conductive chemicals to enhance their selectivity, sensitivity, and stability. Modification of CPEs with conductive materials such as graphene, carbon nanotubes, glassy carbon, metallic nanoparticles, and organic nanomaterials have been reported in the literature. These modifications result in highly differentiated and functionalized surfaces compared to bare CPEs. Graphene, which is a single layer of multiple layers of graphite with high hydrophobicity and excellent conductivity, is one of the most popular CPE modifiers. Polymer materials such as alginate, cellulose, polyaniline, and chitosan have also been frequently used in electrode modifications due to their advantages in chemical and physical stability, conductivity, electrochemical deposition ability, reduced interference in analysis, biocompatibility, and low cost [50, 51]. The addition of conjugated crosslinkers to conjugated conductive polymers further improves their charge transfer features. Modified CPEs are chemically inert, easy to prepare, and allow selective signal enhancement, fast response time, and low residual currents against analyte species in a wide potential range. Furthermore, they can be easily miniaturized and integrated into portable devices, making them ideal for on-

site and point-of-care testing. Electrochemical methods with evolving sensors are increasingly being used in a range of applications in analytical chemistry, including clinical diagnostics, environmental monitoring, and food safety testing, owing to their numerous advantages.

The objective of this research is to develop and validate highly sensitive and selective differential pulse voltammetry (DPV) and cyclic voltammetry (CV) methods for the simultaneous determination of TEV and ETV and to investigate their electrochemical properties. Two new modified carbon paste electrodes (CPEs) were fabricated using graphene nanoplatelets (Gr) and synthesized cross-linked ethylenediamine sulfonamide polymer resin (EDASP) as a modifier. The synthesized EDASP and similar sulfonamide-based polymers have been applied to the sorption and separation of aldehyde [52] and mercury [53] in different matrices. In this study, EDASP was used for the first time in electrode fabrication for voltammetric determination. Gr-CPE and EDASP-CPE sensors were applied to the simultaneous determination of TEV and ETV in tablets with the developed DPV method, and high recovery results ranging from 97.4% to 102.8% were obtained.

## 2. RESULTS AND DISCUSSION

### 2.1. Drug electrochemical behavior and proper electrode fabrication

Modified carbon paste electrode (CPE) is a superior alternative to modified glassy electrodes due to its ease of preparation and replacement, as well as its ability to form sensitive, stable, and selective surface areas with both organic and inorganic compositions of graphite. In this study, various nanomaterials, including graphene, multi-walled carbon nanotubes (MWCNT), and chitosan, synthesized in our laboratory, were tested as carbon paste-modifying materials. An EDASP-modified CPE electrode was also utilized for the first time to examine the substances of drugs. To investigate the electrochemical properties of solutions containing 0.2 mM ETV and 0.2 mM TEV on the prepared electrodes, cyclic voltammetry (CV) measurements were conducted at a scanning rate of 100 mV/s in BR buffer at pH 4.5 over a potential range of 0-1.6 V. The CVs of ETV and TEV displayed well-separated and sharp oxidation peaks at approximately 1.1 V and 1.4V, respectively. No peak was observed in the reverse scan for both compounds.

Figure 1 presents a comparison of the modified CPEs prepared in this study, with DPV voltammograms of bare CPE, 10% MWCNT-CPE, 10% Chitosan-CPE, 10% MgO-CPE, 15% Gr-CPE, and 20% EDASP-CPE recorded in BR pH 4.5 at a scan rate of 20 mV/s of 0.1 mM ETV and 0.1 mM TEV. The results indicate that the Gr-CPE and EDASP-CPE electrodes exhibited the best current response for both drugs among the prepared electrodes.

Compared to the bare CPE, the graphene-modified CPE (Gr-CPE) exhibited a larger electroactive surface area. Furthermore, the shape of the voltammogram was altered by the addition of graphene, resulting in improved separation between the electrode surface oxidation current and the current from ETV and TEV signals. This change facilitated the identification and analysis of the signals from these compounds. The sp<sup>2</sup> hybridization of graphene increases the electroactive surface area of the Gr-CPE electrode by promoting  $\pi$ - $\pi$  interactions between adjacent layers, leading to the formation of hexagonal structures and a consequent increase in surface area [54]. This effect enhances electrode kinetics and improves the electrocatalytic activity of ETV and TEV. Both unmodified and modified electrodes did not display a peak in the backward sweep, indicating that ETV and TEV underwent irreversible oxidation. The electrochemical behavior of ETV and TEV on the water-insoluble resin (EDASP)-modified CPE was comparable to that of the modified Gr-CPE. EDASP was found to have a synergistic effect on the CPE, resulting in a significant improvement in the voltammetric readings of ETV and TEV. The incorporation of EDASP into the CPE electrode resulted in a randomly textured surface and increased the contact area of the CPE composite, providing a highly accessible surface for the oxidation of ETV and TEV, possibly due to the interaction between the resin and drugs.

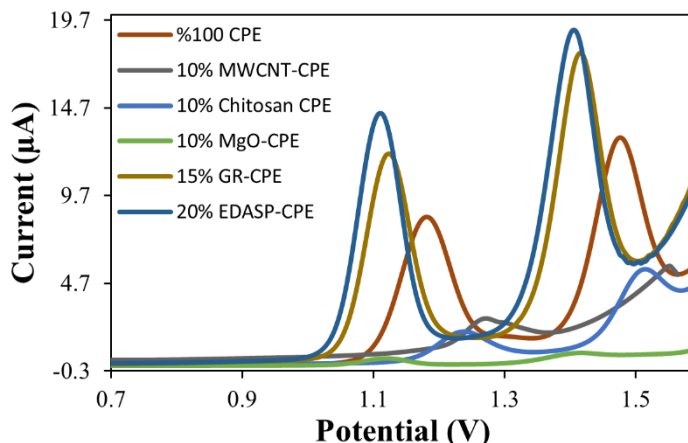


**Figure 1.** DPV (20 mV/s) of 0.1mM solutions of ETV and TEV in pH 4.5 BR buffer on a) 100% CPE, b) 10% MWCNT CPE, c) 10% Chitosan-CPE, d) %10 MgO CPE, e) 15% Gr-CPE, and f) 20% EDASP-CPE.

## 2.2. Determination of the Graphene/EDASP ratio in the CPE

The effect of the graphene and EDASP ratios on the performance of Gr-CPE and EDASP-CPE electrodes with optimal electrochemical responses was evaluated using CV and DPV methods in specific buffer solutions, by measuring the percentage effect. The oxidation signals of ETV and TEV on the surface of Gr-CPE and EDASP-CPE were studied in relation to the content of Gr and EDASP (1.0-25.0%). The results showed that the highest current was obtained when the CPE contained 20% EDASP and 15% graphene, as demonstrated in Figure 2. Compared to the unmodified CPE, the current response obtained with the EDASP-modified electrode was approximately two times higher for ETV and approximately one-third higher for TEV, as shown in Figure 1.

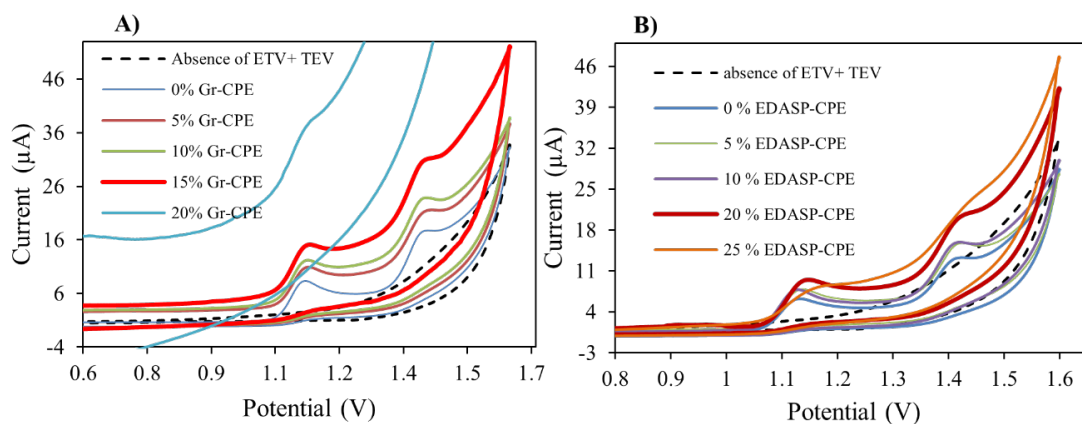


**Figure 2.** CV voltammograms (100mV/s) of 0.1mM ETV and 0.1mM TEV with **A)** Absence of ETV&TEV, 0% Gr-CPE, 5% Gr-CPE, 10% Gr-CPE, 15% Gr-CPE, and 20% Gr-CPE. **B)** Absence of ETV&TEV, 0% EDASP-CPE, 5% EDASP -CPE, 10% EDASP -CPE, 20% EDASP-CPE, and 25% EDASP-CPE.

## 2.3. Effect of pH

### 2.3.1. At Gr-CPE working electrode.

CV and DPV techniques were used to explore a wide range of pH values to determine the ideal electrolyte solution and evaluate how pH affects electrochemical oxidation for the detection of ETV and TEV medicines. In preliminary experiments, the Gr-CPE working electrode was used with CV of 0.2 mM ETV and 0.2 mM TEV solutions in 0.04 M BR buffers with a pH range of 2.0 to 6.0 in the 0-1.600 V operating range, as shown in Figure 3. The  $I_p$  vs pH plot indicated that the current peak increased as the pH value increased until it reached 4.5, after which the oxidation peak current decreased as the pH value continued to increase. At pH

above 6, the current response became too weak to detect due to a reduction in ETV and TEV electron transport. As the strongest signals were recorded at a slightly acidic pH, the next supporting electrolytes tested were phosphate, ammonium acetate, and sodium acetate. The 0.04 M BR buffer solution with pH 4.5 was found to provide the best peak current and was selected as the ideal environment for further research among the solutions tested as electrolyte solutions. The analysis conducted using the CV method in BR solutions with pH 2.0-6.0 revealed that the oxidation process of ETV and TEV was pH dependent. The peak potential gradually shifted towards a more negative potential with an increase in pH, indicating that the protonation of the molecules occurred during the electron transfer process. The correlation between peak potential ( $E_p$ ) and pH (2.0-6.0) was found to be linear, as demonstrated in Figure 3-B1, B2. Both drugs had a slope of approximately 35 mV/pH, as indicated by the equations.

$$\text{For ETV, } E_p \text{ (V)} = -0.0356 \text{ pH} + 1.2226, R^2 = 0.9872$$

$$\text{For TEV, } E_p \text{ (V)} = -0.0354 \text{ pH} + 1.5884, R^2 = 0.9841$$

According to the Nernstian equation the slope of the half-wave potential-pH graph is,

$$\text{Slope} = (59.15p/an) \quad (1)$$

In the equation, "p" represents the total number of protons involved in the reaction, and "n" represents the number of electrons exchanged. The slopes related to ETV and TEV from the plots were 35.4 and 35.6 mV/pH, respectively, which are relatively close to 29.5 mV/pH, indicating that the number of protons released from the molecule during oxidation is half the number of electrons transitioned to the electrode [42, 55-57].

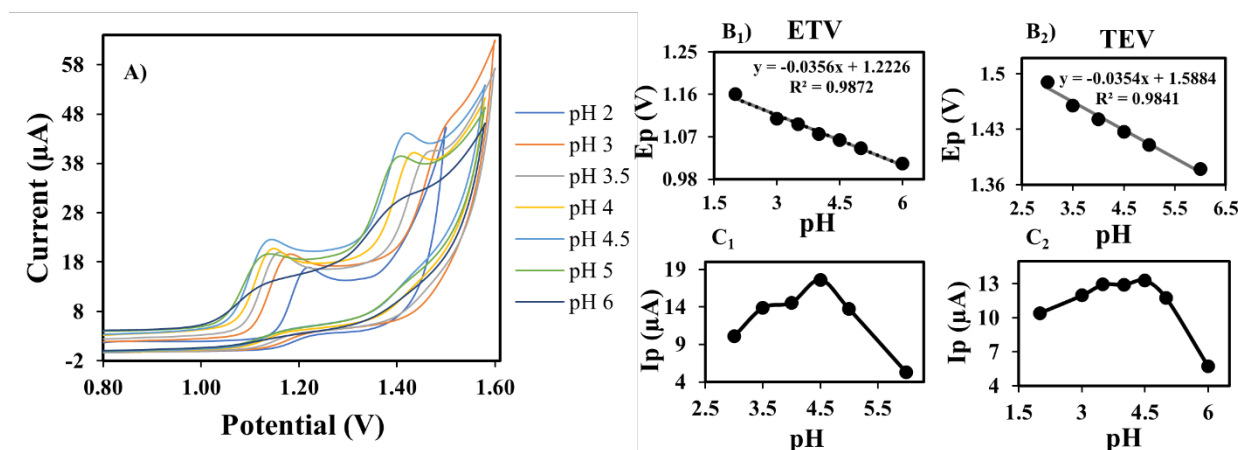


**Figure 3.** (B<sub>1</sub>, B<sub>2</sub>) Influence of pH on the shape of anodic peak at Gr-CPE. (C<sub>1</sub>, C<sub>2</sub>) Influence of pH on the peak current of ETV and TEV.

### 2.3.2. At EDASP-CPE working electrode.

The impact of varying pH levels (2-6) on the electrochemical response of a 0.2 mM solution of ETV and 0.2 mM of TEV on an EDASP-CPE modified electrode is depicted in Figure 4. The reaction was conducted at a scan rate of 100 mV/s and a potential range of 0-1.600 V. The graph shows distinct oxidation peaks for ETV around at 1.1 V and TEV at 1.4 V at each pH level, with the peaks shifting towards less positive values as the pH level increases from 2.0 to 6.0. A graph of current ( $I_p$ ) versus pH was generated and included as an inset in Figure 4c the graph indicates that the highest current response is achieved at a pH of 4.0.

$$\text{For ETV, } E_p = -0.0301 \log v + 1.307, R^2 = 0.9656$$

$$\text{For TEV, } E_p = -0.0289 \log v + 1.561, R^2 = 0.9681$$

The slope of the  $E_p$ -pH relationships for ETV and TEV are 30.1 and 28.9 mV respectively, which implies that the oxidation of ETV and TEV involves transferring an unequal number of electrons and protons, indicating that the oxidation follows the Nernstian equation [55, 57]. As the acidity level decreased, the current at the anode increased (from 6.0 to 3.0). This can be attributed to the protonation of the nitrogen atoms, which are the most basic groups in the molecule [58].

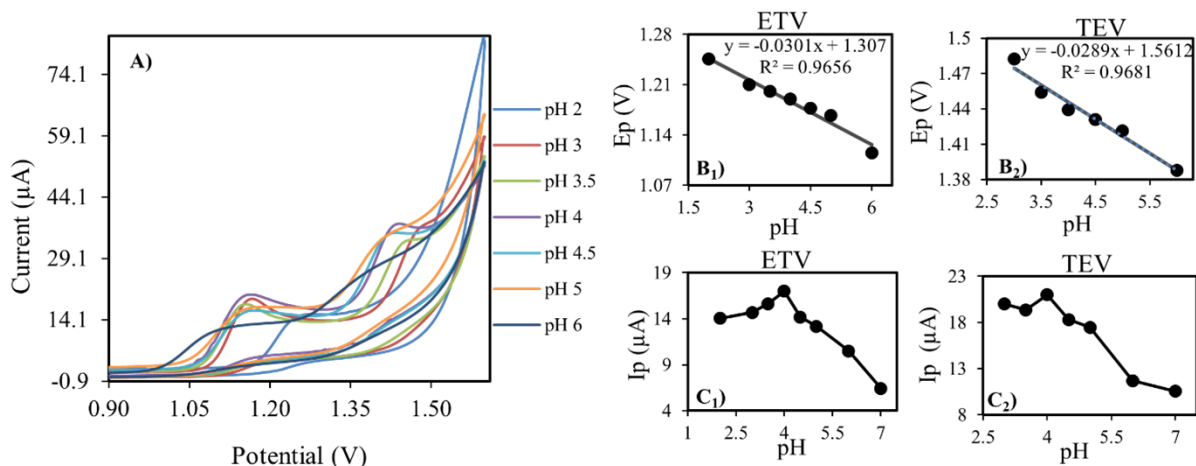


**Figure 4.** (B1, B2) Influence of pH on the shape of anodic peak at EDASP-CPE. (C1, C2) Influence of pH on the peak current of ETV and TEV.

## 2.4. Effect of scan rate

### 2.4.1 Scan rate at Gr-CPE

The electrochemical behavior of ETV and TEV on the Gr-CPE electrode was obtained by taking cyclic voltammograms at a scanning rate of 5- 400 mV/s with a potential range of +0 V to +1.600 V in solutions of 0.2 mM of drugs in BR buffered medium with pH = 4.5. Peak currents and peak potentials were measured and analyzed. As shown in Figure 5, as the scanning rate increased, the oxidation peak current of ETV and TEV steadily increased, and the potential shifted towards a positive potential, indicating that the reaction on the electrode is irreversible. A plot of the logarithm of the peak current in relation to the logarithm of the scanning rate resulted in a linear correlation with a regression equation, as depicted in Figure 5, Inset C. The equations for both compounds are shown as follows:

$$\text{For ETV, } \text{Log} I_p (\mu A) = 0.4315 \log v (Vs^{-1}) + 1.6594, R^2 = 0.9967$$

$$\text{For TEV, } \text{Log} I_p (\mu A) = 0.4597 \log v (Vs^{-1}) + 1.8303, R^2 = 0.9923$$

The slopes of ETV and TEV were 0.4 and 0.5, respectively, which are very close to the predicted value of 0.5 for a clearly diffusion-controlled process [40]. Additionally, the equations that represent the relation between the peak current and the square root of the scan rate are:

$$\text{For ETV, } I_p (\mu A) = 44.98 v^{1/2} (Vs^{-1}) + 2.2395, R^2 = 0.9953$$

$$\text{For TEV, } I_p (\mu A) = 73.344 v^{1/2} (Vs^{-1}) - 0.1813, R^2 = 0.9983$$

The linearity of the  $I_p - v^{1/2}$  curves for both ETV and TEV ( $R^2 = 0.99281$  and  $R^2 = 0.9983$ , respectively) supports the hypothesis that the reaction is controlled by diffusion. This means that the number of particles spreads along the cross-sectional unit from the bulk phase to the interface in proportion to its concentration throughout the area.

The peak potential ( $E_p$ ) of an irreversible process can be expressed by the Laviron equation:

$$E_p = E^\circ + \left( \frac{2.303RT}{anF} \right) \text{Log} \left( \frac{RTK^\circ}{anF} \right) + \left( \frac{2.303RT}{anF} \right) \text{Log} v \quad (2)$$

where  $\alpha$  is the electron transfer coefficient,  $v$  is the scan rate,  $k_0$  is the standard heterogeneous rate constant (cm/s),  $n$  is the number of electrons,  $E_p$  is the peak potential, and  $E_0$  is the official potential found by extending the  $E_p$  - scan rate ( $v$ ) line to  $v = 0$  [41]. The  $\alpha n$  values,  $n$  number, and  $k_0$  values were calculated from the  $E_p$  -  $\log V$  plot. The  $k_0$  values were found to be 159.3 cm/s for ETV and 168.6 cm/s for TEV using the Laviron equation, which indicates that the electron transfer rate of TEV is faster than ETV on the Gr-CPE electrode.

The regression equations obtained from the  $E_p$ - $\log v$  plot were found as:

$$\text{For ETV, } E_p = 0.0272 \log v + 1.1667, R^2 = 0.9703$$

$$\text{For TEV, } E_p = 0.0279 \log v + 1.4614, R^2 = 0.9662$$

The values of  $\alpha n$  for ETV and TEV were calculated by using the slope ( $m$ ) of the equations,

$$\text{Slope} = \left( \frac{2.303RT}{\alpha nF} \right) \quad (3)$$

While  $\alpha n$  values were 2.2 and 2.1, respectively. The  $\alpha$  value for a pH-dependent irreversible reaction can be found by using the equation [40],

$$E_p - E_{p/2} = (47.7/\alpha) \text{ mV}, 25^\circ\text{C} \quad (4)$$

where  $E_{p/2}$  is the half-wave potential where the current is half the peak current [40]. The value of  $\alpha$ , which varies from zero to one for irreversible reactions, was found to be 0.95 and 0.99 for ETV and TEV, respectively, while the  $n$  value was 2.3 and 2.1, corresponding to  $n \approx 2$ .

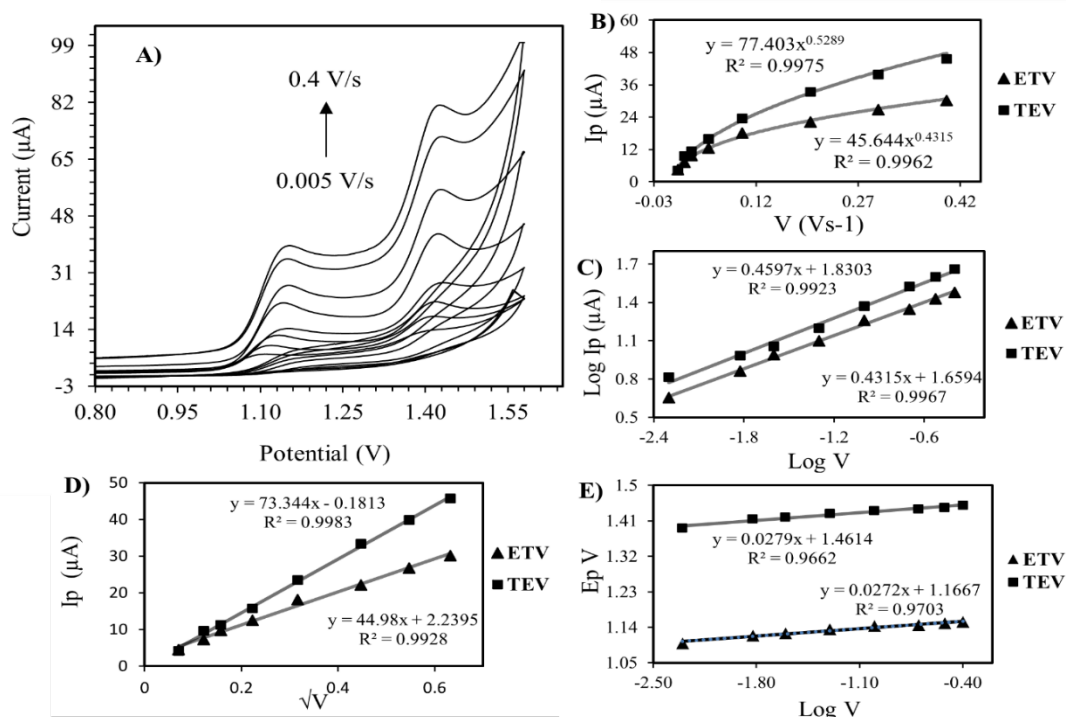


**Figure 5.** (A) Cyclic voltammograms of 0.2 mM ETV and TEV at graphene electrode with different scan rates being from 0.005 to 0.4 Vs<sup>-1</sup>. Inset: (B) Dependence of oxidation peak current on scan rate. (C) Dependence of the logarithm of peak current on logarithm of scan rate. (D) Dependence of oxidation peak current on the square root of scan rate. (E) Dependence of the peak potential on logarithm of scan rate.

#### 2.4.2. Scan rate at EDASP-CPE

The impact of the scanning rate on the oxidation peak current of 0.2 mM ETV and 0.2 mM TEV on the EDASP-CPE electrode was studied under the conditions mentioned above using CV. Figure 6 illustrates the

cyclic voltammograms of 0.2 mM of ETV and TEV in a buffer solution of pH 4.0 on the adjusted electrode at various scanning rates between 0.005 and 0.5 Vs<sup>-1</sup>. The data suggests that the logarithmic graph of peak current (Ip) versus the logarithm of scanning rate (v) and Ip versus (v<sup>1/2</sup>) are linear over the range examined (Figure 6, inset C), as described by the equations:

Log Ip vs. log v:

$$\text{For ETV, } \text{Log } I_p(\mu\text{A}) = 0.4025 \log v (\text{Vs}^{-1}) + 1.5509, R^2 = 0.9958$$

$$\text{For TEV, } \text{Log } I_p(\mu\text{A}) = 0.4412 \log v (\text{Vs}^{-1}) + 1.7761, R^2 = 0.9951$$

Ip vs. v<sup>1/2</sup>:

$$\text{For ETV, } I_p(\mu\text{A}) = 35.146 v^{1/2}(\text{Vs}^{-1}) + 2.4284, R^2 = 0.9953$$

$$\text{For TEV, } I_p(\mu\text{A}) = 61.244 v^{1/2}(\text{Vs}^{-1}) + 1.7441, R^2 = 0.9984$$

In the reverse scan over the potential range studied, only an anodic peak was observed, with no cathodic peak present. This indicates that the oxidation of ETV and TEV on the EDASP-CPE electrode is chemically irreversible, similar to the oxidation reaction observed with the Gr-CPE electrode mentioned previously. The observation of a change in the anodic peak potential towards a higher positive level as the scan rate increases provides additional evidence for the existence of the irreversible oxidation process. The logarithmic graphs of current (Ip) against frequency (v) and Ip against the square root of frequency (v<sup>1/2</sup>) for both substances demonstrate that the oxidation process on the EDASP-CPE and Gr-CPE 257 electrodes is primarily controlled by diffusion.

The values of n and k<sub>0</sub> involved in the reaction were calculated from the relationship between potential and the logarithm of scan rate using the equations provided above in the simultaneous analysis of ETV and TEV using an EDASP-CPE working electrode. The α values for ETV and TEV were calculated as 1.0 and 1.1, respectively, and the n values were calculated as 2.1 and 1.9, which corresponds to about 2. The k<sub>0</sub> values were calculated as 194.4 for ETV and 216.1 for TEV, indicating that the reaction is faster than those obtained with the Gr-CPE electrode. This suggests that the interactions between the analytes and the functional groups of the resin molecules may contribute to the current sensitivity compared to Gr-CPE. This sensitivity is probably due to the interaction of drug and resin groups, providing surface width and contributing to the increase of conductivity.

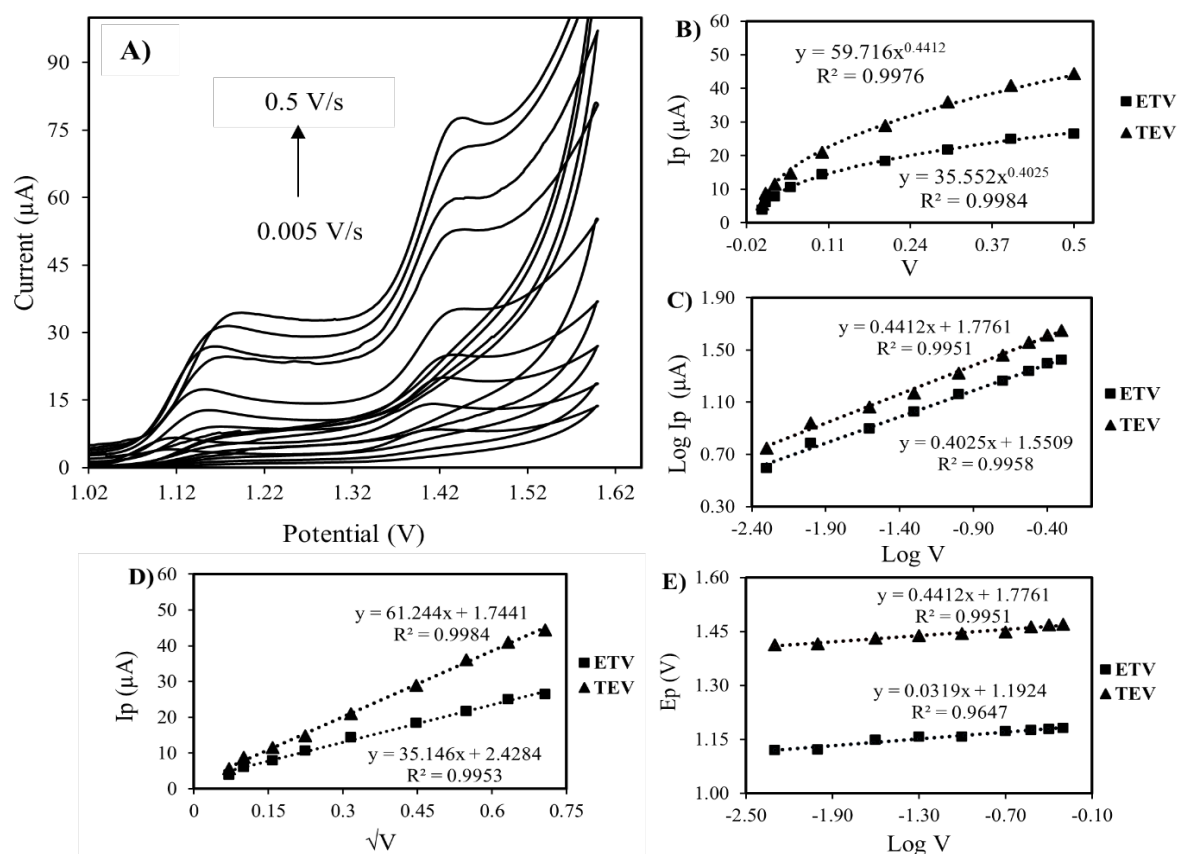


**Figure 6.** (A) Cyclic voltammograms of 0.2 mM ETV and TEV at EDASP electrode with different scan rates being from 0.005 to 0.5 Vs<sup>-1</sup>. Inset: (B) Dependence of oxidation peak current on scan rate. (C) Dependence of the logarithm of peak current on logarithm of scan rate. (D) Dependence of oxidation peak current on the square root of scan rate. (E) Dependence of the peak potential on logarithm of scan rate.

## 2.5. Oxidation mechanism

Fourier transform infrared (FTIR) analyses were conducted on both bulk ETV and TEV compounds, as well as on samples that underwent voltammetric analysis (Figure 7), in order to study their oxidation mechanisms. For this purpose, a weight of 12 mg of each compound was taken separately and dissolved in methanol, the solutions were then diluted with BR buffer. CV scans for each solution were taken repeatedly until the peaks of the compounds were significantly reduced. Electrodes were taken out, drops adhering to its surface were collected and the surface was replaced. The process was repeated until collecting enough amounts. The collected solution was dried with nitrogen gas and sent for analysis.

The FTIR spectral changes between TEV, ETV and their products obtained after the electrode reaction are shown in Figure 7. FT-IR-spectrum of TEV showed small stretch bands at 3203.2 cm<sup>-1</sup> and 2982.4 cm<sup>-1</sup> representing O-H, N-H/C-H functional groups. In the product of TEV, the appearance of a prominent wide band in the range of 3000-3500 cm<sup>-1</sup>, which includes this area, may indicate that additional O-H is formed. In the IR of TEV product, the N-H bending and N-H stretching peaks of primary amines, which are the main peaks of adenine structure, were decreased significantly at 1626.7 cm<sup>-1</sup> and 1253.5 cm<sup>-1</sup>, respectively (Figure 7). Additionally, in the FTIR of the TEV product, the decrease of the peak at 1751.05 cm<sup>-1</sup>, which represents the C=O/C=N functional groups, indicates the structural changes in adenine. In addition, the peak at 1669.1 cm<sup>-1</sup>, which relates to the (R<sub>2</sub>-C=NR) bend in the adenine cycle, disappeared in the spectrum of the TEV product. This suggests that the double bond present in the -N=C- group of the adenine ring underwent oxidation. Furthermore, the FT-IR analysis of the ETV product obtained after the electrode reaction revealed the disappearance of the peaks at 1629 cm<sup>-1</sup> and 1598 cm<sup>-1</sup> in the IR spectra. This suggests that the double bond in the -C=N- group may be replaced by a hydroxyl group, as compared to the IR spectra of the standard ETV.

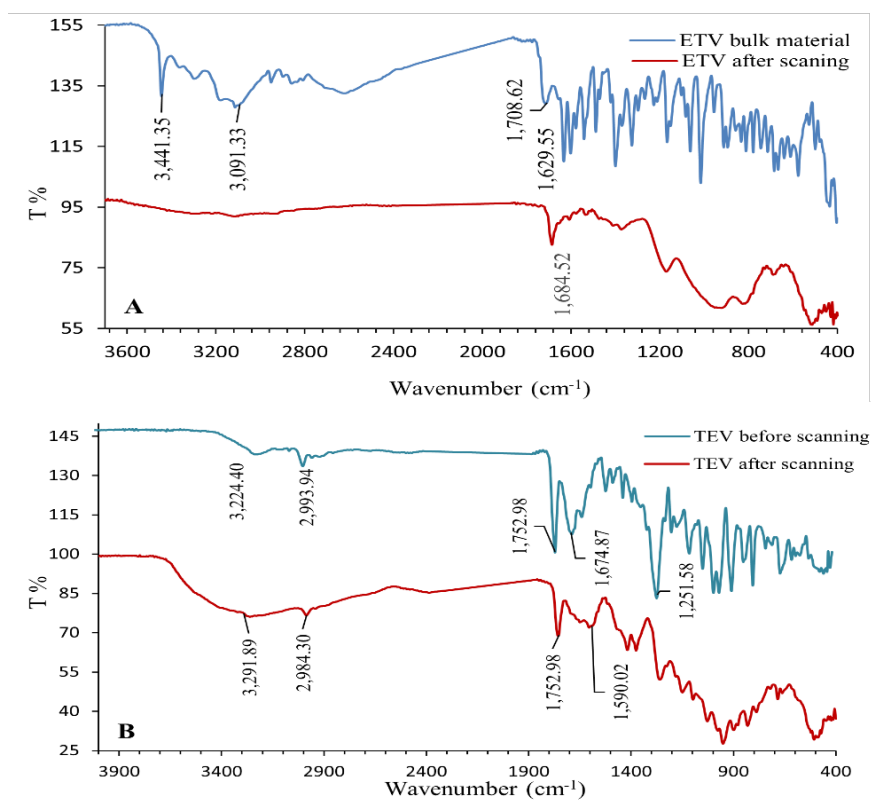


**Figure 7.** (A) FT-IR spectrum of ETV in the bulk materials and after CV scanning (B) FT-IR spectrum of TEV in the bulk materials and after CV scanning.

Previous studies have proposed two different redox mechanisms for TEV, with one mechanism suggesting that the TEV adenine moiety is oxidized at the C2 position to form 2-oxoadenine. This process involves the transferring of 2 electrons and 2 protons, with the 2-electron transfer being the rate-limiting step [40, 43, 59]. The other oxidation mechanism suggested hydroxylation at the C2 position of adenine, resulting in 2-hydroxyadenine [42, 60, 61]. It has been stated here that 2-hydroxyadenine is produced more efficiently in monomers than in polynucleotides [60]. This mechanism involves the transfer of 2 electrons and 1 proton. Similarly, the oxidation of the ETV guanine cycle also follows two pathways. The primary pathway results in the formation of 8-oxoguanine, which requires transfer of equal numbers of electrons and protons, as reported in studies [1, 23]. The alternative pathway, described by [25], involves transfer of 2 electrons and a proton and leads to the formation of 8-hydroxyguanine through hydroxylation at C8.

Based on the above data and the pH-dependent mechanism, we hypothesize that the oxidation mechanism of ETV (Figure 8) and TEV (Figure 8b) at both proposed electrodes follows the formation of 8-hydroxyguanine and 2-hydroxyadenine, respectively, and that the electron number is twice the number of protons. The suggested mechanism is shown in Figure 14.

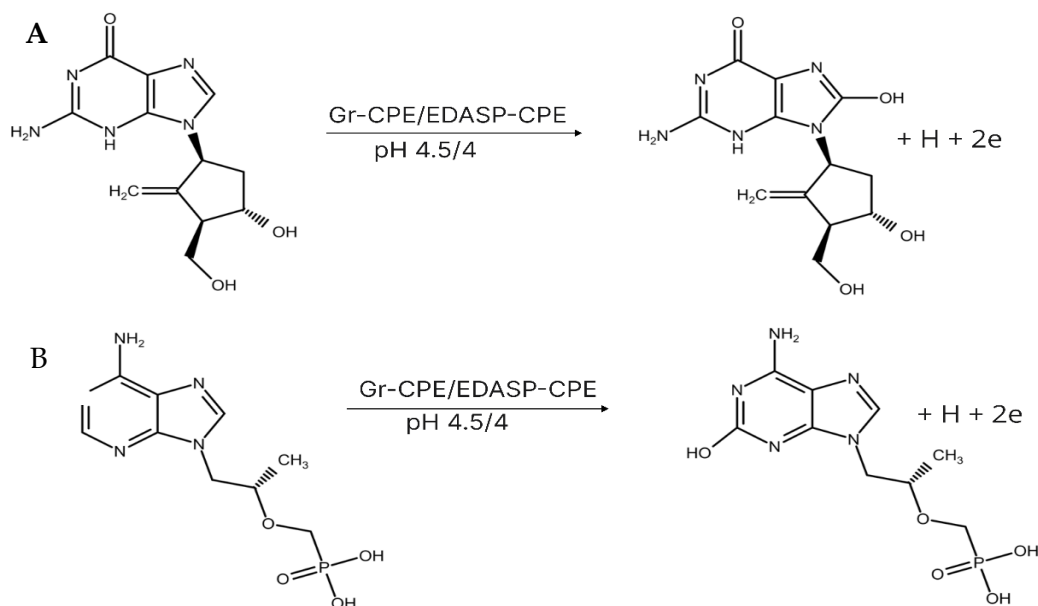


**Figure 8.** Possible oxidation mechanism proposed for TEV and ETV.

While EDASP and graphene have different structures, EDASP, depicted in figure14, exhibits an interconnected structure through intermolecular interactions, specifically sulfonamide-amine, amine-amine, and sulfonamide-sulfonamide interactions, that shares some similarities with the sp<sup>2</sup> structure of graphene electrode material [61, 62]. This process enhances the electroactive surface area of the electrode, leading to improved kinetics and enhanced electrocatalytic activity towards ETV and TEV. Another study suggests that sulfonamide resin may play a role in forming slightly stable radicals (R-SO<sub>2</sub>-N.CH<sub>2</sub>CH<sub>2</sub>NH<sub>2</sub> or R-SO<sub>2</sub>-NHCH<sub>2</sub>CH<sub>2</sub>N.H) under acidic conditions (pH of 4.0), with TEV potentially interacting with the amine group of the resin through its phosphoric acid function, and ETV possibly interacting with either the sulfonamide or amine radical [62, 63]. This interaction may result in electrostatic interactions such as N-H...O=P, O-H...O=S, and N-H...O=S.

## 2.6. SEM analysis

In addition to the FT-IR structure characterization, the morphology and elemental composition of modified electrodes were examined by SEM-EDX spectroscopy. SEM images of the EDASP resin, Gr-CPE, and EDASP-doped CPE electrodes are presented in Figure 9 and Figure 10. In the characterization of SEM-EDX, according to Figure 9. A, the EDASP resin has a spherical form, but irregular particles and cracks were observed because of exothermic reaction conditions and mechanical deformations. However, it was revealed that 1 μm and 10 μm diameter Gr-CPE (Figure 9A and B) and 10 μm diameter EDASP-CPE (Figure 10B) electrode materials exhibit similar structures, their morphological structures are large, fuzzy-edged, layered semi-amorphous particles and porous. In contrast, SEM image of 100 nm diameter EDASP-CPE and 200 μm diameter Gr-CPE exhibited suitable smooth surfaces with a large active surface area, non-uniform, distorted superimposed foam-cloud-like structure size and distribution (Figure 9C, Figure 10C). The modified electrodes exhibited a synergistic composition with good dispersion of Gr and EDASP in graphite, allowing for high sensitivity measurements of both molecules.

The elemental composition of the graphene-doped carbon paste was analyzed using EDX spectroscopy, revealing a carbon-to-oxygen atom ratio of 91.9% to 8.1%, respectively (Figures 9 and 10). This higher carbon ratio and lower oxygen ratio than expected for graphite [63] suggests successful modification. The EDX spectrum of EDASP-CPE revealed the presence of nitrogen and sulfur atoms, which are suitable for the sulfonamide polymer structure. The "C and O" atom ratios were also found to be reasonable. These results indicate the successful modification of the electrode materials with nanomaterials.

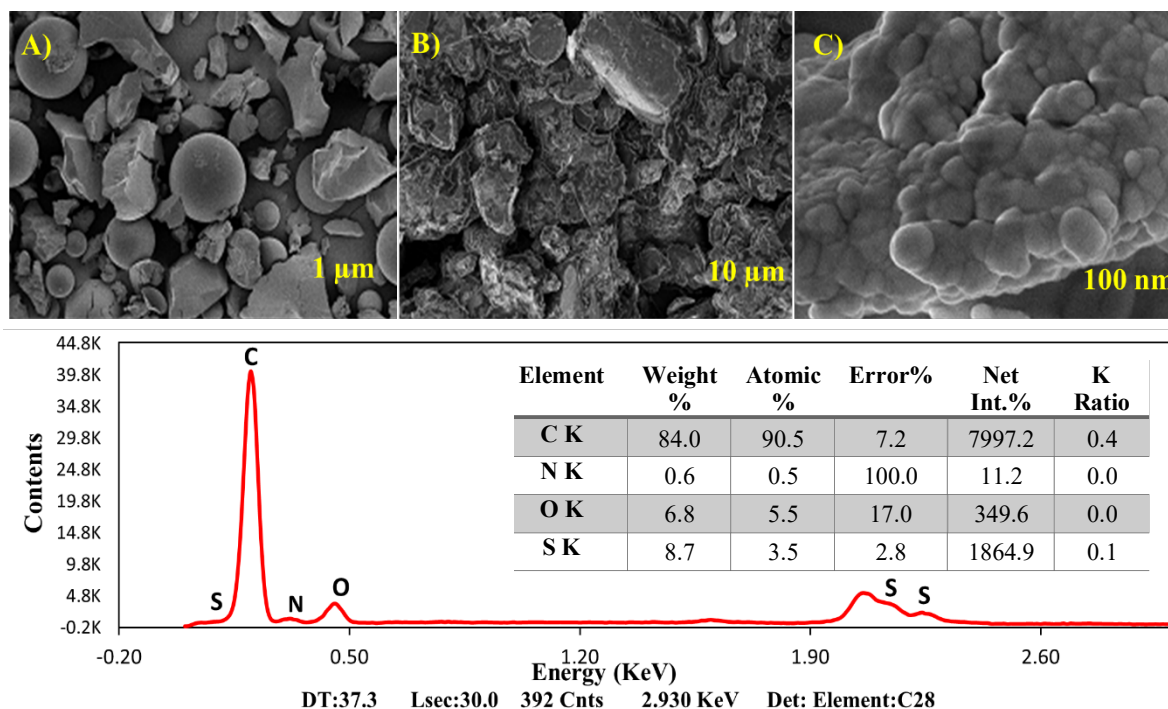


**Figure 9.** SEM images of (a) 1 μm (b) 10 μm, (c) 200 nm Graphene-doped CPE electrodes and its EDX analysis report.

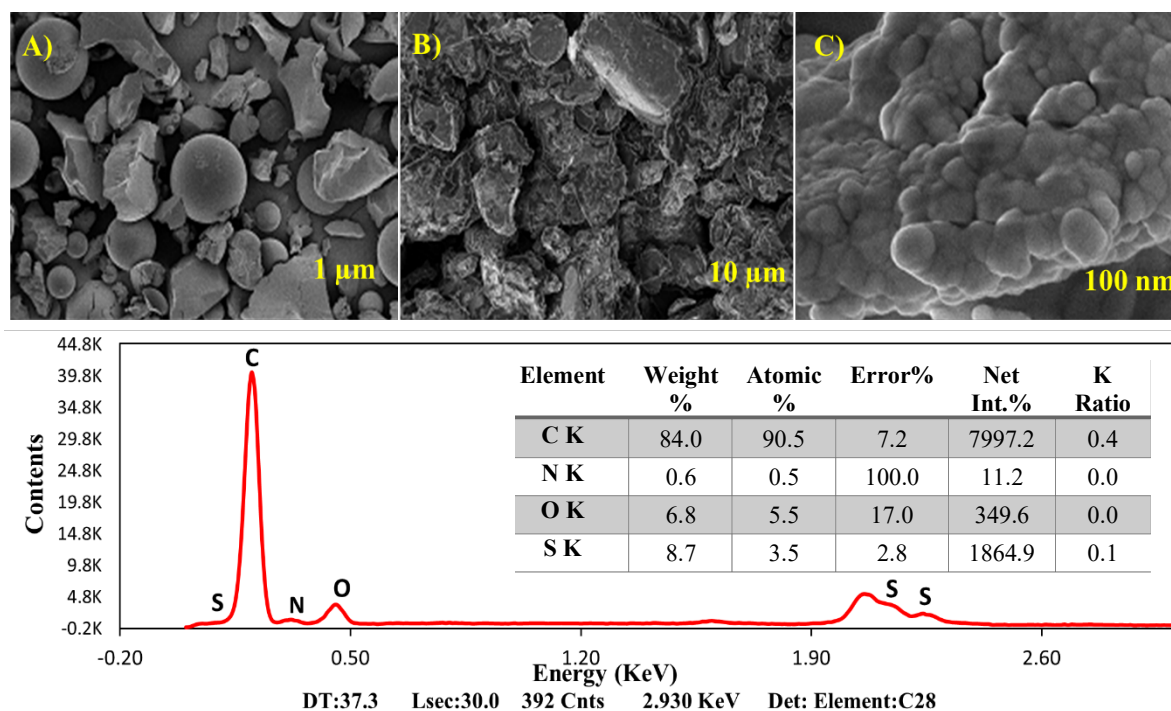


**Figure 10.** SEM images of (A) 1 μm pure EDASP resin (B) 10 μm EDASP-CPE, (C) 200nm EDASP-CPE electrodes and EDASP-CPE EDX analysis report.

## 2.7. Method validation

### 2.7.1. Linearity and sensitivity

The DPV method was used to quantify ETV and TEV at graphene and EDASP electrodes. DPV was chosen as it produces more accurate peaks at lower concentrations of ETV and TEV than cyclic voltammetry,

and results in a reduced baseline current, leading to better resolution. The study found that DPV can be employed to measure the levels of ETV and TEV at pH 4.0 and 4.5 using the specified electrolyte. Figure 11 illustrates a linear correlation between the current peak and the concentrations of ETV and TEV, as demonstrated using differential pulse voltammograms. Using the above-mentioned ideal conditions, a linear dynamic range for ETV and TEV, from 1.0 to 250.0  $\mu\text{M}$ , was obtained on both electrodes, as shown in Table 1. Limit of detection (LOD) values for ETV and TEV were 0.2  $\mu\text{M}$ , while limits of quantitation (LOQ) were 0.6 and 0.7  $\mu\text{M}$  respectively, at Gr-CPE.

The LOD of ETV and TEV on EDASP-CPE were 0.2  $\mu\text{M}$ , and LOQ values were 0.5 and 0.7  $\mu\text{M}$ , respectively, as shown in Table 1 and Figure 12. The statistical information for the calibration curves was obtained from six individual measurements, and the LOD and LOQ were established by utilizing the provided equations.

$$LOD = \frac{3s}{m}; LOQ = \frac{10s}{m}$$

The equations used to calculate LOD and LOQ take into account the standard deviation of the current peak response and the slope of the calibration curve ( $s$  and  $m$ , respectively) [65]. When evaluating the slope of the calibration curve and the closeness of the measurements, which are among the sensitivity parameters, were evaluated, it was observed that both substances showed excellent sensitivity with the modified electrodes, although the TEV response was slightly higher.

**Table 1.** Statistical parameters for determination of ETV and TEV determination at Gr-CPE and EDASP-CPE electrodes by DPV method.

Parameters	ETV at Gr-CPE	TEV at Gr-CPE	ETV at EDASP-CPE	TEV at EDASP-CPE
Peak Potential (V)	~1.1	~1.4	~1.1	~1.4
Linearity ( $\mu\text{M}$ )	1.0-250.0	1.0-250.0	1.0-250.0	1.0-250.0
Slope <sup>a</sup>	$6.9 \times 10^{-2}$	$7.5 \times 10^{-2}$	$6 \times 10^{-2}$	$7.8 \times 10^{-2}$
Intercept	0.1305	0.1411	0.1441	0.1415
LOD ( $\mu\text{M}$ )	0.2	0.2	0.2	0.2
LOQ ( $\mu\text{M}$ )	0.6	0.7	0.5	0.7
SE of slope <sup>b</sup>	$1.6 \times 10^{-5}$	$2.1 \times 10^{-5}$	$6.9 \times 10^{-5}$	$2.2 \times 10^{-5}$
SE of intercept	$1.8 \times 10^{-3}$	$2.4 \times 10^{-3}$	$7.8 \times 10^{-4}$	$2.5 \times 10^{-3}$
Correlation coefficient (r)	0.9996	0.9998	1	0.9997

<sup>a</sup> $y(\mu\text{A}) = mC(\mu\text{M}) + b$ ;  $y$  is current peak height,  $m$  is slope,  $b$  is intercept

<sup>b</sup>SE: Standard Error

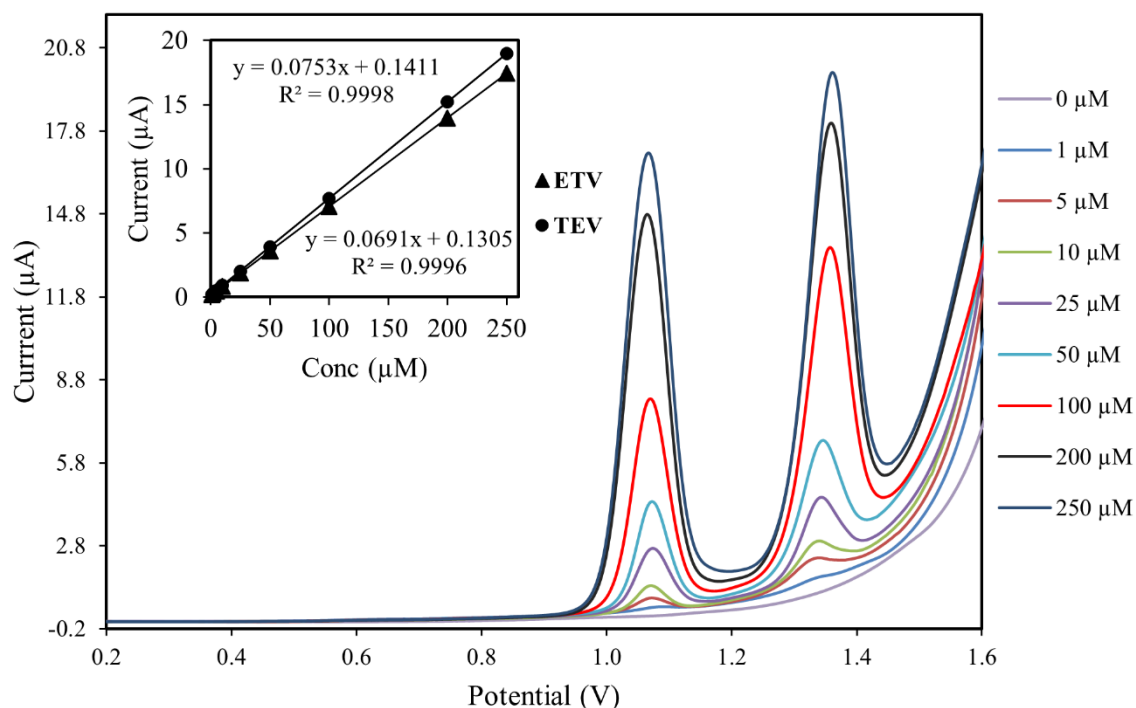


**Figure 11.** Differential-pulse voltammograms of ETV and TEV using Graphene electrode at pH 4.5 buffer solution at different concentrations: 1, 5, 10, 25, 50, 100, 200 and 250µM. Inset: Plot of the peak current against the concentration of ETV and TEV.

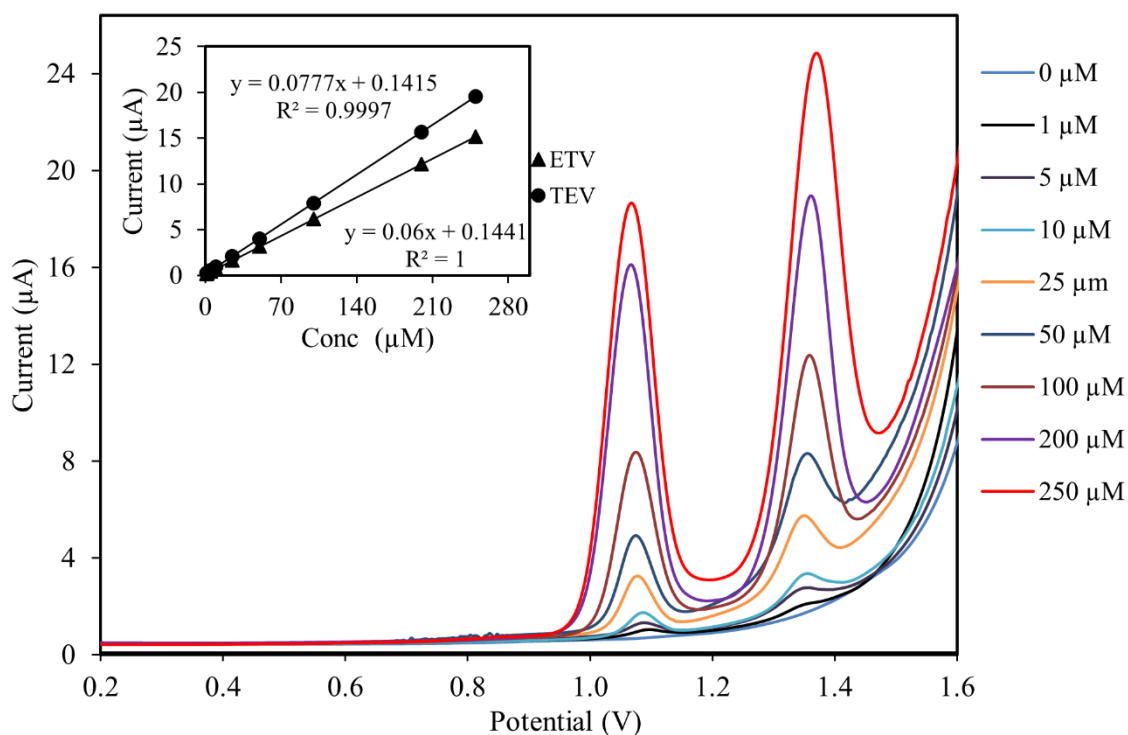


**Figure 12.** Differential-pulse voltammograms of ETV and TEV using EDASP electrode at pH 4.0 buffer solution at different concentrations: 1, 5, 10, 25, 50, 100, 200 and 250µM. Inset: Plot of the peak current against the concentration of ETV and TEV.

### 2.7.2. Accuracy and precision

The intra-day (repeatability) and inter-day precision (reproducibility) of the proposed DPV method were evaluated by measuring ETV and TEV at both electrodes at three different concentrations (20, 50, and 100  $\mu\text{M}$ ) within the linear dynamic range. Repeatability was calculated by taking five consecutive measurements at the expressed concentrations on the same day, yielding an average percent relative standard deviation (RSD) of 0.9% to 3.8% for both drugs, indicating good repeatability of the method (Table 2). For reproducibility, fresh electrodes were prepared each time, and the analysis was conducted at the same concentrations over a period of five days within a two-week period. High precision was obtained with RSDs in the mean range of 0.9% to 3.4% for both drugs (Table 2). The calculated Horwitz ratios (HorRat), which indicate the acceptability of the assay test, were also calculated. The results showed excellent precision with average HorRat values of 0.1 and 0.6 for intra-day and inter-day studies, respectively (Table 2) [65].

Additionally, the accuracy test, which gives the closeness of the measured value to the true value, was obtained by the recovery of the analyte added to the blind matrix. The accuracy of developed methods was evaluated using the same samples of drugs for both electrodes. Average percent recovery values of accuracy for ETV and TEV were obtained with Gr-CPE electrode between 95.7-102.6% and with EDASP-CPE between 99.8-101.8% (Table 2).

Also, the % recovery and %RSD parameters were compared with the data of voltammetric studies reported in the literature. Accordingly, the %RSD values obtained for the determination of TEV were lower than some previous studies [44, 66]. Likewise, the % recovery values of drugs were compared, and similar results were found with some existing ones, but higher than some voltammetric studies by Festinger and Chihava [41, 43] for the TEV determination method; Elqudaby [23] for ETV determination method. All these data prove that the proposed DPV methods are highly precise and accurate, making them a valuable tool for the combined determination of ETV and TEV in clinical and pharmaceutical applications.

**Table 2.** Analytical precision and accuracy of ETV and TEV determination at Gr-CEP and EDASP-CPE electrodes by DPV method.

		Gr-CEP					EDASP-CPE				
		Added ( $\mu\text{M}$ )	Found ( $\mu\text{M}$ ) $\pm\text{SD}$	Recovery (%)	RSD (%)	Hor Rat <sup>a</sup>	Added ( $\mu\text{M}$ )	Found ( $\mu\text{M}$ ) $\pm\text{SD}$	Recovery (%)	RSD (%)	Hor Rat <sup>a</sup>
ETV	Intra-day	20	19.2 $\pm$ 0.7	96.1	3.8	0.6	10	10.0 $\pm$ 0.2	100.1	1.8	0.2
		50	51.0 $\pm$ 0.5	102.1	1.0	0.2	25	25.5 $\pm$ 0.4	101.8	1.6	0.2
		100	100.0 $\pm$ 1.0	100.0	1.0	0.2	50	49.9 $\pm$ 0.5	99.8	1.0	0.2
	Inter-day	20	20.1 $\pm$ 0.7	100.7	3.4	0.3	10	10.1 $\pm$ 0.3	100.5	3.4	0.2
		50	51.3 $\pm$ 0.5	102.6	0.9	0.1	25	25.0 $\pm$ 0.5	100.0	1.9	0.1
		100	100.0 $\pm$ 1.3	100.0	1.3	0.1	50	49.9 $\pm$ 0.8	99.8	1.6	0.1
TEV	Intra-day	20	19.3 $\pm$ 0.7	96.6	3.8	0.6	10	10.1 $\pm$ 0.3	100.9	2.6	0.3
		50	49.9 $\pm$ 0.6	99.8	0.9	0.2	25	25.5 $\pm$ 0.4	101.8	1.6	0.3
		100	95.9 $\pm$ 1.1	95.9	1.2	0.2	50	50.6 $\pm$ 0.7	101.1	1.5	0.3
	Inter-day	20	19.4 $\pm$ 0.6	97.0	3.3	0.2	10	10.2 $\pm$ 0.3	101.5	3.3	0.2
		50	49.6 $\pm$ 0.9	99.2	1.8	0.2	25	25.1 $\pm$ 0.6	100.2	3.2	0.2
		100	95.7 $\pm$ 1.6	95.7	1.6	0.2	50	50.4 $\pm$ 0.6	100.7	1.2	0.1

HorRat = RSD/Predicted PRSD, the predicted relative standard deviation (among-laboratory) (PRSDR =  $2C^{-0.15}$ ).

### 2.7.3. Electrode stability and reproducibility

To evaluate the repeatability of the proposed sensors, five measurements were taken using DPV from a solution containing 50  $\mu\text{M}$  of ETV and TEV on the same day. The results showed that the Gr-CPE electrode had an RSD of 2.9% for ETV and 3.5% for TEV, while the EDASP-CPE electrode had an RSD of 2.5% for ETV and 1.8% for TEV, indicating that the sensors have a high level of repeatability. The reproducibility of the developed sensors was also evaluated by independently fabricating five different electrodes and measuring ETV and TEV concentrations of 50  $\mu\text{M}$  over an 8-week period, as shown in Figure 13. The results showed that the sensors exhibited acceptable reproducibility, with RSDs of 3.5% and 3.8% for ETV and TEV, respectively, using the Gr-CPE electrode, and RSDs of 2.7% and 2.0% using the EDASP-CPE electrode (Table 3).

**Table 3.** Electrode stability and reproducibility were tested over 8 weeks taking 50  $\mu\text{M}$  ETV and 50  $\mu\text{M}$  TEV at Gr-CPE and EDASP-CPE.

Studied compounds	Gr-CPE			EDASP-CPE		
	Conc.( $\mu\text{M}$ )	$I_p(\text{mA})^a \pm \text{SD}$	RSD (%)	Conc.( $\mu\text{M}$ )	$I_p(\text{mA})^a \pm \text{SD}$	RSD (%)
ETV	50	3.9 $\pm$ 0.1	3.5	50	3.5 $\pm$ 0.1	2.7
TEV	50	3.1 $\pm$ 0.1	3.8	50	4.0 $\pm$ 0.1	2.0

a: average of 8 weeks currents measuring for 7 repeating each.

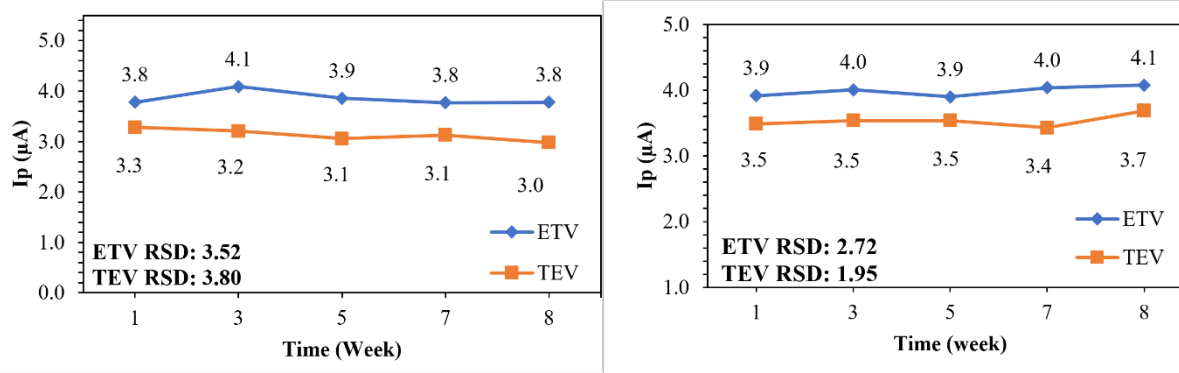


**Figure 13.** Reproducibility of electrode stability over 8 weeks ( $n=7$ ) of Gr-CPE (a) and EDASP-CPE (b) electrode respectively at 50  $\mu\text{M}$  for each ETV and TEV in BR buffer.

#### 2.7.4. Selectivity and effect of excipients

The potential impact of excipients commonly found in pharmaceutical formulations or body fluids on the proposed analytical method was investigated. Sample solutions containing the same amount of ETV and TEV (50 $\mu\text{M}$ ) in a BR buffer mixed with significant amounts of each excipient were analyzed under the same experimental conditions to examine their effect on the voltammetric response. The results, shown in Table 4, indicated that a hundred-fold excess of  $\text{Na}^+$ ,  $\text{K}^+$ ,  $\text{Ca}^{2+}$ , glucose, starch, and ten-fold of vitamin C (ascorbic acid) did not affect the voltammetric response. The potential of TEV showed only a slight change of more than 5% when only citric acid was present without effecting the potential respond of ETV, indicating that the analysis of ETV and TEV can be performed in the presence of these excipients, making it specific and selective. The high recovery in the presence of interferences not only reinforces the method's accuracy but also suggests that the methods can be applied to determine both drugs in biological matrices.

#### 2.7.5 Determination of ETV and TEV in tablets

The developed DPV methods were employed to determine the ETV and TEV content simultaneously in tablet samples using two fabricated working electrodes. The content of the tablets was determined by using the current values in the regression equation established with the ETV and TEV standard solutions, and the recoveries were determined. Results were determined by averaging the results of 5 separate analyses. The average recovery of ETV in tablets using the DPV method was 98.9% at the Gr-CPE electrode and 97.4% at the EDASP-CPE electrode. The average recovery of TEV in tablets was found to be 102.8% at the Gr-CPE electrode and 101.3% at the EDASP-CPE electrode. At the same time, both drugs were determined separately in their tablets by DPV method at 2 different concentrations to confirm whether the drug mixture was determined correctly from the TEV tablet and whether the combined analysis had any effect. When the results of simultaneous and separate determination of drugs in tablets were examined, it was revealed that there was no significant difference in terms of %RSD values and recovery results (Table 5) and samples had a content level between 97.4% and 102.8% of the mean in their simultaneous determinations and between 100.0 and 102.0 in their separate analyses. These results are within the threshold of 95-115%, indicating that both antiviral drugs can be safely determined together in combined tablet preparations.

**Table 4.** Influence of potential excipients on the voltammetric response of 50  $\mu$ M ETV and 50  $\mu$ M TEV at Gr-CEP and EDASP-CPE.

Excipients	Concentration of Excipients /mM	Ip of ETV in the absence of Excipient	Ip of ETV in the presence of Excipient	Signal change (%)	Ip of TEV in the absence of Excipient	Ip of TEV in the presence Of Excipient	Signal change (%)
Graphene-CPE							
Na+	5mM	3.4	3.3	-2.1	3.5	3.6	1.4
K+	5mM	3.3	3.3	-1.2	3.5	3.4	-3.1
Glucose	5mM	3.4	3.4	2.4	3.6	3.5	-2.0
Starch	5mM	3.4	3.3	-2.4	3.6	3.7	3.9
Lactic acid	5mM	3.3	3.2	-1.8	3.6	3.4	-3.9
Ascorbic acid	0.5mM	3.4	3.4	1.2	3.6	3.7	2.8
Citric acid	0.5mM	3.4	3.5	3.1	3.5	3.2	-8.9
EDASP-CPE electrode							
Na+	5mM	3.4	3.3	-4.4	3.5	3.4	-4.3
K+	5mM	3.5	3.4	-2.9	3.6	3.7	2.2
Glucose	5mM	3.4	3.5	1.2	3.6	3.6	2.0
Starch	5mM	3.4	3.3	-3.5	3.5	3.7	3.7
Lactic acid	5mM	3.5	3.6	2.6	3.5	3.5	-1.4
Ascorbic acid	0.5mM	3.4	3.3	-5.0	3.5	3.4	-4.0
Citric acid	0.5mM	3.5	3.4	-2.9	3.5	3.2	-8.5

**Table 5.** Results of simultaneous and separate determination of ETV and TEV in pharmaceutical formulations by DPV method (n=5).

Studied compounds	Gr-CPE				EDASP-CPE			
	Tablet taken(mg)	Found(mg) $\pm$ SD	Recovery (%)	RSD (%)	Tablet taken(mg)	Found(mg) $\pm$ SD	Recovery (%)	RSD (%)
<b>Simultaneous determination of ETV and TEV from tablets</b>								
ETV	14.9	14.8 $\pm$ 0.5	98.9	3.6	14.9	14.5 $\pm$ 0.5	97.4	3.5
TEV	141.5	145.5 $\pm$ 6.7	102.8	4.6	141.5	143.4 $\pm$ 5.8	101.3	4.1
<b>Separate determination of ETV and TEV from tablets</b>								
ETV	0.5	0.5 $\pm$ 0.0	102.0 $\pm$ 6.5	4.3	0.5	0.5 $\pm$ 0.0	100.2 $\pm$ 4.0	4.0
ETV	1.0	0.5 $\pm$ 0.1	100.8 $\pm$ 4.7	4.6	1.0	0.5 $\pm$ 0.0	100.0 $\pm$ 4.1	4.1
TFV	200.0	201.0 $\pm$ 7.3	100.5 $\pm$ 3.7	3.6	200.0	201.0 $\pm$ 4.7	100.5 $\pm$ 2.4	2.4
TFV	245.0	248.7 $\pm$ 10.7	101.5 $\pm$ 4.4	4.3	245.0	246.9 $\pm$ 7.0	100.8 $\pm$ 2.8	2.8

### 3. CONCLUSION

In this study, new and effective CV and DPV techniques based on the use of Gr-CPE and EDASP-CPE were developed for the first time to simultaneously determine ETV and TEV and to investigate their electrochemical properties. For the first time, EDASP resin nanomaterial was used as an electrode material in the modification of the carbon paste electrode. Under the same experimental conditions, carbon paste electrodes modified with Gr and EDASP showed quite high sensitivity in determination of both drugs compared to bare CPE. The effect of scanning rate and pH were investigated to obtain the highest response for detailed electro analysis of ETV and TEV. Electrochemical studies show that both substances are irreversible and diffusion-controlled, involving the transport of one proton and two electrons. The experiments were conducted using a 0.04 M Britton-Robinson buffer as the supporting electrolyte with a pH of 4 for Gr-CPE and a pH of 4.5 for EDASP-CPE. The electrode reactions of the substances were examined by

CV, DPV, and FTIR techniques. The SEM morphological analysis revealed the successful modification of the electrode surface with EDASP resin and Gr. The Gr-CPE and EDASP-CPE electrodes showed clear oxidation peaks for ETV and TEV at approximately 1.1 V and 1.4 V respectively. The DPV technique was used to measure the linear increase of current responses for ETV and TEV at concentrations between 1.0 and 250.0  $\mu\text{M}$  on Gr-CPE and EDASP-CPE electrodes. LOD values were 0.2  $\mu\text{M}$  for both studies. Excellent selectivity and performance have been achieved without interacting with many excipients that can be found in pharmaceutical preparations and biological fluids. The fabricated Gr-CPE and EDASP-CPE sensors offered highly selective, sensitivity, good stability, and high conductivity, and were applied to the simultaneous detection of ETV and TEV in tablets with high recoveries using the DPV method. These superior properties make it possible to accurately determine the substances in biological matrices.

Although various methods have been developed for the detection and quantification of antiviral drugs, including TEV and ETV, LOD/LOQ values were found to be less sensitive than the current study and the detection linear ranges were generally narrower. Among these there are spectrophotometry, chromatography, and electrochemistry methods. ETV was determined at 437 nm and 293.6 nm by spectrophotometric methods, with a linear range of 1.4-6.8  $\mu\text{M}$  [15] and 1.7-17.0  $\mu\text{M}$  [18] and LODs of 0.5  $\mu\text{M}$  and 0.06  $\mu\text{M}$ , respectively. TEV was determined at a range of wavelengths around 229-260 nm, with linear ranges of 1.7-139.3  $\mu\text{M}$  [29], 17.4-174.1  $\mu\text{M}$  [30], and 7.0-139.3  $\mu\text{M}$  [31] and LODs of 0.04  $\mu\text{M}$ , 1.6  $\mu\text{M}$ , and 1.5  $\mu\text{M}$ , respectively. Some studies have investigated the development of electrochemical nanosensors for the detection of ETV and TEV individually. In ETV electrochemical determinations, DPV, SWV, LSV and SWCAdSV methods are used. Composition of the used working electrodes are GCE [23], NiFe<sub>2</sub>O<sub>4</sub>-IL/CPE [25] and CeO<sub>2</sub>-GONRs/GCE [1]. The linear ranges vary according to the method, range from 2.2 -32.4  $\mu\text{M}$ , 0.5-100  $\mu\text{M}$  and 0.08 -2.2  $\mu\text{M}$  and 2.2-155  $\mu\text{M}$  and LODs are 0.6  $\mu\text{M}$ , 0.04  $\mu\text{M}$  and 0.002  $\mu\text{M}$  respectively. Similarly, TEV is quantified using DPV, SWV and SWCAdSV methods. Main electrodes used are Bare GCE [38], HMDE [37], dsDNA/BDD [39], GO/GCE [43], Ag-BAC/GCE [40], Ni-CoS/GQDs/GCE [41], NiS@PAA-MWCNT/GCE [42] and MIP-Pt@g-C<sub>3</sub>N<sub>4</sub>/F-MWCNT/SPE [45]. The linear range are 0.6-60  $\mu\text{M}$ , 1.7-17  $\mu\text{M}$ , 5-100  $\mu\text{M}$ , 0.3-30  $\mu\text{M}$ , 0.06-1.0  $\mu\text{M}$ , 5-18  $\mu\text{M}$ , 20-80  $\mu\text{M}$ , 0.7-100  $\mu\text{M}$  and 0.005-0.7  $\mu\text{M}$  while the LOD are 0.1  $\mu\text{M}$ , 0.5  $\mu\text{M}$ , 0.6  $\mu\text{M}$ ,  $4.8 \times 10^{-3} \mu\text{M}$ ,  $2.4 \times 10^{-3} \mu\text{M}$ ,  $1.2 \times 10^{-5} \mu\text{M}$ ,  $5.6 \times 10^{-5} \mu\text{M}$ , 0.2  $\mu\text{M}$  and 0.003  $\mu\text{M}$  respectively. In the meanwhile, very few methods have reported simultaneous determination of ETV and TEV, including HPLC-UV and HPLC-MS/MS methods. Detection in HPLC-UV was carried out at 255 nm with linear ranges of  $0.9 \times 10^{-2}$  -0.3 and 0.9-3.4  $\mu\text{M}$  and LODs of  $0.9 \times 10^{-2}$  and 0.9  $\mu\text{M}$ , respectively [46]. In HPLC-MS/MS [47], the LODs for ETV and TEV are  $0.7 \times 10^{-4}$  and 0.03  $\mu\text{M}$ , respectively.

In summary, the proposed method has several advantages over other complicated instrumental analysis techniques, including the elimination of pre-assay sample preparation, high sensitivity, fast response, good reproducibility, and requires a small amount of material. These findings show that the DPV method developed with the newly designed Gr-CPE and EDASP-CPE electrodes is a sensitive, selective, and accurate option for analysis of ETV and TEV in preparations at very low concentrations.

## 4. MATERIALS AND METHODS

### 4.1. Chemicals

Graphite powder with a particle size of less than 20  $\mu\text{m}$  and chitosan (Cs) were obtained from Sigma-Aldrich. Graphene nanoplatelets (Gr; 5-10 nm; specific surface area 750 m<sup>2</sup>/g; diameter 5-10  $\mu\text{m}$ ) and multi-walled carbon nanotubes (MWCNT; for general purposes) were supplied by Nanografi. Ethylenediamine sulfonamide polymer resin was manufactured at the Department of Chemistry at Istanbul Technical University. TEV and ETV were obtained from Sanovellaç (Istanbul, Turkey) and were used as received. Paraffin wax (56-58, in pastille form), methanol, and acetonitrile were obtained from Merck. The other chemicals were ordered from Riedel de Haen. These include sulfuric acid (H<sub>2</sub>SO<sub>4</sub>), glacial acetic acid (CH<sub>3</sub>COOH), boric acid (H<sub>3</sub>BO<sub>3</sub>), orthophosphoric acid (H<sub>3</sub>PO<sub>4</sub>), and potassium chloride (KCl) of analytical grade, which was used without purification.

Standard solutions of ETV and TEV were made by dissolving the compounds at a concentration of 10 mM in methanol and stored at 4°C until use in the assay. Working solutions with concentrations ranging from 1.0 to 250.0  $\mu\text{M}$  were made by diluting the standard solutions with methanol immediately before each use. A range of universal Britton-Robinson buffer (BR) with pH values of 2-8 was utilized as the supporting electrolyte. The Britton-Robinson buffers were made by blending 0.04 M boric acid, 0.04 M phosphoric acid, and 0.04 M acetic acid, which were then modified to the appropriate pH range of 2-8 with 0.2 M sodium hydroxide [67].

## 4.2. Apparatus

Electrochemical analyses were carried out using a computer-controlled BASi Epsilon-EC version 2 potentiostat systems (Bioanalytical Systems, Inc., West Lafayette, IN). A standard three-electrode cell with a volume of 25 mL was used: Ag/AgCl (3M NaCl) electrode (MF-2052, BASi) as the reference electrode (RE), a platinum wire counter electrode (CE). The Gr-CPE and EDASP-CPE served as the working electrodes (WE). Fourier transform infrared (FTIR) spectra were obtained in the 4000–650  $\text{cm}^{-1}$  spectrum using a Bruker Alpha Universal Attenuated total reflection (ATR) sampling accessory spectroscope (GmbH, Germany). Graphene and cross-linked ethylenediamine sulfonamide polymer resin-modified CPE were featured by field emission scanning electron microscopy, FE-SEM (ZEISS Sigma 300, Germany) with energy dispersive X-ray spectrometry (EDX). pH measurements were employed with a pH ion meter (Mettler Toledo) and pure water used obtained by an ultra-pure water device (Purelab Option).

## 4.3 Synthesis of cross-linked ethylenediamine sulfonamide polystyrene resin (EDASP)

The synthesis of ethylenediamine polystyrene resin (Figure 14) was reported by Biçak and Şenkal (1997) and then by Yavuz et al. (2015). Briefly, the preparation of cross-linked chlorosulfonated polystyrene resin was started by mixing styrene (90% mol) and divinyl benzene (DVB) (10% mol) monomers with dibenzoyl peroxide in toluene and polymerizing at 80 °C for 8 h using the suspension polymerization method. After washing and drying, this crosslinked polystyrene resin was chlorosulfonated using excess chlorosulfonic acid (approximately 50 mL) for 2 h at 0°C and 18 h at room temperature. This reaction mixture was poured into the ice-water mixture and stirred. The chlorosulfonated resin was then filtered and cleaned. In the final step, 10 g of chlorosulfonated polystyrene (CSPS) resin was reacted with an excess of ethylenediamine (12 mL) in 30 ml of 2-methyl pyrrolidone at 0 °C, followed by continuous shaking for 24 h at room temperature. The reaction contents were filtered in an aqueous solution, washed, and dried under vacuum to yield the final product, (EDASP).

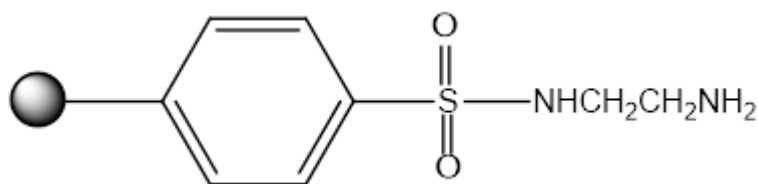


Figure 14. Structure of EDASP

## 4.4. Preparation of modified electrochemical electrodes

To prepare the best sensor for simultaneous determination of ETV and TEV, carbon paste electrodes were prepared using various modifiers. After the appropriate modifiers were selected, their proper components were studied and optimized.

For fabricated modified electrodes, 5-25% graphene (GR), 5-25% cross-linked ethylenediamine sulfonamide polymer resin (EDASP), 10% multi-walled carbon nanotubes (MWCNT), 10% chitosan and 10% MgO were weighed separately, as modifiers. 75%-95% graphite was added to make up the total electrode material powder to 100% and thoroughly blended by a spatula in a glass beaker, and then blended with paraffin wax melted at a 3:10 weight ratio (paraffin: electrode material) at 70 °C for about 25 minutes. A small portion of the prepared paste was firmly filled into the hole (2.87 mm) at the end of a commercial plastic disc electrode body (BASi MF-2010, 7.5 cm x 3.4 mm) and polished by rolling it on a clean sheet of paper to ensure a perfectly smooth surface. Unmodified CPE (bare CPE) was obtained by mixing 1 g of graphite with 0.3 g of melted paraffin wax and applying the same procedure. When the electrode surface needs to be renewed, the old one is removed by a spatula, the electrode body is washed with water and alcohol, and a new paste is placed and polished in the same way. Also, before each experiment, the electrode surface was smoothed and rinsed with distilled water.

The prepared CPE pastes were stored in tightly closed glass containers in the dark at room temperature. Prior to analysis, the electrode was immersed in a BR buffer solution, and voltammograms were registered to ensure stability.

#### 4.5. Working dynamic range

In the simultaneous determination of ETV and TEV, various experimental parameters such as operating potential range and scanning speed were studied for current optimization. All experiments were conducted at room temperature. The electrochemical behavior of ETV and TEV on selected modified Gr-CPE and EDASP-CPE was investigated with CV against Ag/AgCl at a scanning rate of 100 mV/s in the potential range between 0-1.6V. For drug determination using differential pulse voltammetry (DPV) analysis, the potential window was chosen between 0.0 and 1.6 V, starting from zero. DPV measurements were performed using a 50 ms pulse width, 50 mV pulse amplitude, 4 mV step potential (Estep), 100  $\mu$ A sensitivity, and a 20 mV/s scanning rate. The oxidation current peak values of approximately 1.1V for ETV and 1.3-1.4 V for TEV were recorded in the voltammogram.

The experimental procedure was as follows: 10 mL of 0.1 M BR buffer (pH 4.0 or pH 4.5) was added to a Pyrex cell, and DPVs of the empty solution were recorded. Then, for the working dynamic range, eight different concentrations of ETV and TEV (from 1.0 to 500  $\mu$ M) were prepared, and peak currents were measured after mixing. The peak current values were recorded against the concentrations of the added compounds, and a calibration curve was plotted. The regression equation of the curve was determined, and at least 6 measurements were conducted for each concentration. The developed method was then used to analyze the substances in the tablets.

#### 4.6. Assay of tablets

TEV Tablets (245 mg TEV per tablet, Voxus®) were obtained from a local market and produced by Sanovelliç (Istanbul, Turkey). Five tablets of TEV were finely powdered, and one tablet's equivalent weight was taken. Since a commercial combination of ETV and TEV in tablet form is not available, 14.7 mg of ETV was mixed with this weighed TEV tablet powder. The mixture of ETV and TEV was transferred to a 100 mL volumetric flask and blended with about 70 mL of methanol. The solution was then sonicated for 1 h, diluted to 100 volumes with methanol, and filtered. Appropriate quantities of the solutions were measured and evaluated using DPV. The concentration of the active ingredient in the tablet was determined using the regression equations established for the corresponding standard drugs. TEV in its pure form was considered the base in the calculation rather than its ester form as a prodrug.

To monitor whether there were any effects or deviations in the application of the developed DPV method to the determination of both drugs simultaneously in tablets, it was also applied separately to the determinations of commercial tablets containing ETV and TEV. Hepagard tablet (1 mg ETV per tablet) containing ETV and Voxus tablet (245 mg TEV per tablet) containing TEV were prepared in methanol as described above, and their determinations were made separately in the same manner.

**Acknowledgements:** This study has been made from the doctoral thesis of Adel Asfoor (Istanbul University, Institute of Graduate Studies in Health Sciences). This study was supported by Istanbul University Scientific Research Projects Unit. Project code: TDK-2020-20398.

#### REFERENCES

- [1] Asran AM, Mohamed MA, Ahmed N, Banks CE, Allam NK. An innovative electrochemical platform for the sensitive determination of the hepatitis B inhibitor Entecavir with ionic liquid as a mediator. *J Mol Liq.* 2020; 302: 112498. <https://doi.org/10.1016/j.molliq.2020.112498>
- [2] Guvenir M, Arikan A. Hepatitis B Virus: From Diagnosis to Treatment. *Pol J Microbiol.* 2020; 69(4): 391-399. <https://doi.org/10.33073/pjm-2020-044>
- [3] Yeh ML, Huang CF, Huang CI, Holmes JA, Hsieh MH, Tsai YS, Liang PC, Tsai PC, Hsieh MY, Lin ZY, Chen SC, Huang JF, Dai CY, Chuang WL, Chung RT, Yu ML. Hepatitis B-related outcomes following direct-acting antiviral therapy in Taiwanese patients with chronic HBV/HCV co-infection. *J Hepatol.* 2020; 73(1): 62-71. <https://doi.org/10.1016/j.jhep.2020.01.027>
- [4] Pawlotsky JM, Negro F, Aghemo A, Berenguer M, Dalgard O, Dusheiko G, Marra F, Puoti M, Wedemeyer H. European Association for the Study of the Liver. EASL recommendations on treatment of hepatitis C: Final update of the series. *J Hepatol.* 2020; 73(5): 1170-1218. <https://doi.org/10.1016/j.jhep.2020.08.018>
- [5] Huang P, Wang Y, Yue M, Ge Z, Xia X, Jeyarajan AJ, Holmes JA, Yu R, Zhu C, Yang S, Lin W, Chung RT. The risk of hepatitis C virus recurrence in hepatitis C virus-infected patients treated with direct-acting antivirals after achieving

- a sustained virological response: A comprehensive analysis. *Liver Int.* 2021; 41(10): 2341-2357. <https://doi.org/10.1111/liv.14976>
- [6] Chien RN, Liaw YF. Current trend in antiviral therapy for chronic hepatitis B. *Viruses.* 2022; 14(2):434. <https://doi.org/10.3390/v14020434>
- [7] Shiffman ML. Approach to the patient with chronic hepatitis B and decompensated cirrhosis. *Liver Int.* 2020; 40(S1):22-26. <https://doi.org/10.1111/liv.14359>
- [8] Lim YS, Seto WK, Kurosaki M, Fung S, Kao JH, Hou J, Gordon SC, Flaherty JF, Yee LJ, Zhao Y, Agarwal K, Lampertico P. Review article: Switching patients with chronic hepatitis B to tenofovir alafenamide-a review of current data. *Aliment Pharmacol Ther.* 2022; 55(8): 921-943. <https://doi.org/10.3390/v12090998>
- [9] Ma X, Liu S, Wang M, Wang Y, Du S, Xin Y, Xuan S. Tenofovir alafenamide fumarate, tenofovir disoproxil fumarate and entecavir: Which is the most effective drug for chronic hepatitis B? A systematic review and meta-analysis. *J Clin Transl Hepatol.* 2021; 9(3): 335-344. <https://doi.org/10.14218/JCTH.2020.00164>
- [10] Lee IC, Lan KH, Su CW, Li CP, Chao Y, Lin HC, Hou MC, Huang YH. Efficacy and renal safety of prophylactic tenofovir alafenamide for HBV-infected cancer patients undergoing chemotherapy. *Int J Mol Sci.* 2022;23(19):11335. <https://doi.org/10.3390/ijms231911335>
- [11] Wang Y, Wang L, Chen X, Sun C, Zhu Y, Kang Y, Zeng S. Chiral detection of entecavir stereoisomeric impurities through coordination with R-besivance and Zn(II) using mass spectrometry. *J Mass Spectrom.* 2018; 53(3): 247-256. <https://doi.org/10.1002/jms.4060>
- [12] Kim YJ. Chapter 27 - Antiviral drugs. In: Ray SD, editor. *Side Effects of Drugs Annual*, 43th ed., Elsevier, 2021, pp323-328. <https://doi.org/10.1016/bs.seda.2021.09.007>
- [13] Marino A, Cosentino F, Ceccarelli M, Moscatt V, Pampaloni A, Scuderi D, D'Andrea F, Rullo EV, Nunnari G, Benanti F, Celesia BM, Cacopardo B. Entecavir resistance in a patient with treatment-naïve HBV: A case report. *Mol Clin Oncol.* 2021;14(6):113. <https://doi.org/10.3892/mco.2021.2275>
- [14] Rizwana BF, Prasana JC, Abraham CS, Muthu S. Spectroscopic investigation, hirshfeld surface analysis and molecular docking studies on anti-viral drug entecavir. *J Mol Liq.* 2018; 1164:447-458. <https://doi.org/10.1016/j.molstruc.2018.03.090>
- [15] Babu NR, Padmavathi Y, Kumar PR, Babu RS, Vijaya DV, Polker A. Development of new spectrometric method for estimation of entecavir monohydrate in formulation using 3-amino phenol as chromogenic reagent. *J Pharm Sci Res.* 2019; 11(6): 2452-2457.
- [16] Naz A, Tabish I, Naseer A, Siddiqi AZ, Siddiqui FA, Mirza AZ. Green chemistry approach: Method development and validation for identification and quantification of entecavir using FT-IR in bulk and pharmaceutical dosage form. *Futur J Pharm Sci.* 2021; 7:75. <https://doi.org/10.1186/s43094-021-00211-9>
- [17] Deodhe ST, Dhabarde DM, Kamble MA, Mahapatra DK. Development and validation of a novel stability indicating RP-HPLC method for the estimation of Entecavir in tablet formulation. *Eur J Anal Chem.* 2017; 12(3): 223-235. <https://doi.org/10.12973/ejac.2017.00165a>
- [18] El-Sayed HM, Abdel Fattah LE, Abdellatef HE, Hegazy MA, Abd El-Aziz MM. Selective Determination of entecavir in the presence of its oxidative degradate by spectrophotometric and chromatographic methods. *J AOAC Int.* 2021; 104(3): 847-853. <https://doi.org/10.1093/jaoacint/qsab015>
- [19] Zhang D, Fu Y, Gale JP, Aubry AF, Arnold ME. A sensitive method for the determination of entecavir at picogram per milliliter level in human plasma by solid phase extraction and high-pH LC-MS/MS. *J Pharm Biomed Anal.* 2009; 49(4): 1027-1033. <https://doi.org/10.1016/j.jpba.2009.02.003>
- [20] Challa BR, Awen BZ, Chandu BR, Rihanaparveen S. LC-ESI-MS/MS method for the quantification of entecavir in human plasma and its application to bioequivalence study. *J Chromatogr B Analyt Technol Biomed Life Sci.* 2011; 879(11-12): 769-776. <https://doi.org/10.1016/j.jchromb.2011.02.023>
- [21] Vlckova H, Janak J, Gottvald T, Trejtnar F, Solich P, Novakova L. How to address the sample preparation of hydrophilic compounds: Determination of entecavir in plasma and plasma ultrafiltrate with novel extraction sorbents. *J Pharm Biomed Anal.* 2014; 88: 337-344. <https://doi.org/10.1016/j.jpba.2013.08.034>
- [22] De Nicolo A, Bonifacio G, Boglione L, Cusato J, Pensi D, Tomasello C, Di Perri G, D'Avolio A. UHPLC-MS/MS method with automated on-line solid phase extraction for the quantification of entecavir in peripheral blood mononuclear cells of HBV+ patients. *J Pharm Biomed Anal.* 2016; 118:64-69. <https://doi.org/10.1016/j.jpba.2015.10.017>
- [23] Elqudaby H, Hendawy H, Zayed M. Microdetermination of entecavir drug in its pharmaceuticals forms and in biological fluids using anodic voltammetry. *World J Pharm. Res.* 2014; 7:1115-1120.

- [24] Jhankal K, Sharma A, Sharma D. Quantification of antiviral drug entecavir in pharmaceutical formulation by voltammetric techniques. *World J Pharm Res.* 2015; 7(1): 10.
- [25] Tandel RD, Naik RS, Seetharamappa J. Electrochemical characteristics and electroensing of an antiviral drug, entecavir via synergic effect of graphene oxide nanoribbons and ceria nanorods. *Electroanalysis.* 2017; 29(5): 1301-1309. <https://doi.org/10.1002/elan.201600492>
- [26] Pinto Neto LFdS, Bassetti BR, Fraga IHV, Oliveira Santos CR, Ximenes PD, Miranda AE. Nephrotoxicity during tenofovir treatment: A three-year follow-up study in a Brazilian reference clinic. *Braz J Infect Dis.* 2016; 20(1):14-18. <https://doi.org/10.1016/j.bjid.2015.09.004>
- [27] Gennaro A, Remington-The Science and Practice of Pharmacy, 20th ed., Vol. 1., Lippincott Williams and Wilkins, Maryland, USA, 2000.
- [28] Moffat AC, Osselton MD, Widdop B, Watts J. Clarke's analysis of drugs and poisons, 4th ed., Pharmaceutical press, London, 2011.
- [29] AbdelHay MH, Gazy AA, Shaalan RA, Ashour HK. Simple Spectrophotometric methods for determination of tenofovir fumarate and emtricitabine in bulk powder and in tablets. *J Spectrosc (Hindawi).* 2013; 2013: 937409. <https://doi.org/10.1155/2013/937409>
- [30] Yunoos M, Praveen TD, Manikanta P, Sai AK, Mounica V, Siva D. A simple validated UV spectrophotometric method for the estimation of tenofovir disoproxil fumarate in bulk and pharmaceutical dosage form. *Res J Pharm Technol.* 2015; 8(4): 365-368. <https://doi.org/10.5958/0974-360X.2015.00061.X>
- [31] Ashour HK, Belal TS. New simple spectrophotometric method for determination of the antiviral mixture of emtricitabine and tenofovir disoproxil fumarate. *Arab J Chem.* 2017; 10: S1741-S1747. <https://doi.org/10.1016/j.arabjc.2013.06.024>
- [32] Pu F, Pandey S, Bushman LR, Anderson PL, Ouyang Z, Cooks RG. Direct quantitation of tenofovir diphosphate in human blood with mass spectrometry for adherence monitoring. *Anal Bioanal Chem.* 2020; 412: 1243-1249. <https://doi.org/10.1007/s00216-019-02304-0>
- [33] Abdelhay M, Gazy A, Shaalan R, Ashour H. Selective RP-HPLC DAD method for determination of tenofovir fumarate and emtricitabine in bulk powder and in tablets. *Acta Chromatographica.* 2015; 27(1): 41-54. <https://doi.org/10.1556/AChrom.27.2015.1.4>
- [34] Ramaswamy A, Dhas ASAG. Development and validation of analytical method for quantitation of emtricitabine, tenofovir, efavirenz based on HPLC. *Arab J Chem.* 2018; 11(2): 275-281. <https://doi.org/10.1016/j.arabjc.2014.08.007>
- [35] Simiele M, Carcieri C, De Nicolò A, Ariaudo A, Sciandra M, Calcagno A, Bonora S, Di Perri G, D'Avolio A. A LC-MS method to quantify tenofovir urinary concentrations in treated patients. *J Pharm Biomed Anal.* 2015; 114: 8-11. <https://doi.org/10.1016/j.jpba.2015.05.001>
- [36] Prathipati PK, Mandal S, Destache CJ. Simultaneous quantification of tenofovir, emtricitabine, rilpivirine, elvitegravir and dolutegravir in mouse biological matrices by LC-MS/MS and its application to a pharmacokinetic study. *J Pharm Biomed Anal.* 2016; 129: 473-481. <https://doi.org/10.1016/j.jpba.2016.07.040>
- [37] Jain R, Sharma R. Cathodic adsorptive stripping voltammetric detection and quantification of the antiretroviral drug tenofovir in human plasma and a tablet formulation. *J Electrochem Soc.* 2013; 160(8): H489. <https://doi.org/10.1149/2.105308jes>
- [38] Ozcelikay G, Dogan-Topal B, Ozkan SA. Electrochemical characteristics of tenofovir and its determination in dosage form by electroanalytical methods. *Rev Roum Chim.* 2017; 62(6-7): 569-578.
- [39] Morawska K, Popławski T, Ciesielski W, Smarżewska S. Electrochemical and spectroscopic studies of the interaction of antiviral drug Tenofovir with single and double stranded DNA. *Bioelectrochem.* 2018; 123: 227-232. <https://doi.org/10.1016/j.bioelechem.2018.06.002>
- [40] Ozcelikay G, Dogan-Topal B, Ozkan SA. An electrochemical sensor based on silver nanoparticles-benzalkonium chloride for the voltammetric determination of antiviral drug tenofovir. *Electroanalysis.* 2018; 30(5):943-954. <https://doi.org/10.1002/elan.201700753>
- [41] Chihava R, Apath D, Moyo M, Shumba M, Chitsa V, Tshuma P. One-pot synthesized nickel-cobalt sulfide-decorated graphene quantum dot composite for simultaneous electrochemical determination of antiretroviral drugs: lamivudine and tenofovir disoproxil fumarate. *J Sens.* 2020; 2020: 3124102. <https://doi.org/10.1155/2020/3124102>
- [42] Alake J, Nate Z, Adu DK, Ike BW, Chauhan R, Karpoormath R. Facile one-step synthesis of nickel sulphide nanoparticles decorated poly (acrylic acid) coated multi-walled carbon nanotube for detection of tenofovir in human urine. *Electrocatalysis.* 2022; 14:232-246. <https://doi.org/10.1007/s12678-022-00784-w>

- [43] Festinger N, Spilarewicz-Stanek K, Borowczyk K, Guziejewski D, Smarzewska S. Highly sensitive determination of Tenofovir in pharmaceutical formulations and patients urine – Comparative electroanalytical studies using different sensing methods. *Molecules*. 2022; 27(6): 1992. <https://doi.org/10.3390/molecules27061992>
- [44] Zeng W, Xiao J, Yao L, Wei Y, Zuo J, Li W, Ding J, He Q. Lanthanum doped zirconium oxide-nanocomposite as sensitive electrochemical platforms for Tenofovir detection. *Microchem J*. 2022; 183: 108053. <https://doi.org/10.1016/j.microc.2022.108053>
- [45] Mehmandoust M, Soylak M, Erk N. Innovative molecularly imprinted electrochemical sensor for the nanomolar detection of Tenofovir as an anti-HIV drug. *Talanta*. 2023; 253:123991. <https://doi.org/10.1016/j.talanta.2022.123991>
- [46] Altaf H, Ashraf M, Hayat MM, Hussain A, Shahzad N, Ahmad B, Rahman J. HPLC method for simultaneous determination of entecavir and tenofovir in human spiked plasma and pharmaceutical dosage forms. *Lat Am J Pharm*. 2015; 34(3): 126-130.
- [47] De Nicolò A, Simiele M, Pensi D, Boglione L, Allegra S, Di Perri G, D'Avolio A. UPLC-MS/MS method for the simultaneous quantification of anti-HBV nucleos (t) ides analogs: Entecavir, lamivudine, telbivudine and tenofovir in plasma of HBV infected patients. *J Pharm Biomed Anal*. 2015; 114: 127-132. <https://doi.org/10.1016/j.jpba.2015.05.016>
- [48] Zhao F-J, Tang H, Zhang Q-H, Yang J, Davey AK, Wang J-P. Salting-out homogeneous liquid-liquid extraction approach applied in sample pre-processing for the quantitative determination of entecavir in human plasma by LC-MS. *J Chromatogr B Analyt Technol Biomed Life Sci*. 2012; 881: 119-125. <https://doi.org/10.1016/j.jchromb.2011.12.003>
- [49] Caldevilla R, Morais SL, Cruz A, Delerue-Matos C, Moreira F, Pacheco JG, Santos M, Barroso MF. Electrochemical chemically based sensors and emerging enzymatic biosensors for antidepressant drug detection: A review. *Int J Mol Sci*. 2023; 24(10): 8480. <https://doi.org/10.3390/ijms24108480>
- [50] Boumya W, Taoufik N, Achak M, Barka N. Chemically modified carbon-based electrodes for the determination of paracetamol in drugs and biological samples. *J Pharm Anal*. 2021; 11(2): 138-154. <https://doi.org/10.1016/j.jpha.2020.11.003>
- [51] Katowah DF, Mohammed GI, Al-Eryani DA, Osman OI, Sobahi TR, Hussein MA. Fabrication of conductive cross-linked polyaniline/G-MWCNTS core-shell nanocomposite: A selective sensor for trace determination of chlorophenol in water samples. *Polym Adv Technol*. 2020; 31(11): 2615-2631. <https://doi.org/10.1002/pat.4988>
- [52] Biçak N, Şenkal BF. Aldehyde separation by polymer-supported oligo (ethyleneimines). *J Polym Sci Part A: Polym Chem*. 1997; 35(14):2857-2864. [https://doi.org/10.1002/\(SICI\)1099-0518\(199710\)35:14<2857::AID-POLA6>3.0.CO;2-N](https://doi.org/10.1002/(SICI)1099-0518(199710)35:14<2857::AID-POLA6>3.0.CO;2-N)
- [53] Yavuz E, Turan GT, Alkazan S, Senkal BF. Preparation of crosslinked quaternary amide-sulfonamide resin for removal of mercury ions from aqueous solutions. *Desalination Water Treat*. 2015; 56(8): 2145-2153. <https://doi.org/10.1080/19443994.2014.958539>
- [54] Wang Y, Hsine Z, Sauriat-Dorizon H, Mlika R, Korri-Youssoufi H. Structural and electrochemical studies of functionalization of reduced graphene oxide with alkoxyphenylporphyrin mono- and tetra- carboxylic acid: application to DNA sensors. *Electrochim Acta*. 2020; 357: 136852. <https://doi.org/10.1016/j.electacta.2020.136852>
- [55] Awad MI, Sayqal A, Pashameah RA, Hameed AM, Morad M, Alessa H, Shah RK, Akassem M. Enhanced paracetamol oxidation and its determination using electrochemically activated glassy carbon electrode. *Int J Electrochem Sci*. 2021; 16(1): 150864. <https://doi.org/10.20964/2021.01.12>
- [56] Kissinger P, Heineman WR. *Laboratory Techniques in Electroanalytical Chemistry*, second ed., CRC press, New York, USA 2018. <https://doi.org/10.1201/9781315274263>
- [57] Gaba M, Mohan C. Development of drugs based on imidazole and benzimidazole bioactive heterocycles: recent advances and future directions. *Med Chem Res*. 2016; 25: 173-210. <https://doi.org/10.1007/s00044-015-1495-5>
- [58] Shen H, Choi C, Masa J, Li X, Qiu J, Jung Y, Sun Z. Electrochemical ammonia synthesis: Mechanistic understanding and catalyst design. *Chem*. 2021; 7(7): 1708-1754. <https://doi.org/10.1016/j.chempr.2021.01.009>
- [59] Kamiya H, Kasai H. Formation of 2-hydroxydeoxyadenosine triphosphate, an oxidatively damaged nucleotide, and its incorporation by DNA polymerases. Steady-state kinetics of the incorporation. *J Biol Chem*. 1995; 270(33): 19446-19450. <https://doi.org/10.1074/jbc.270.33.19446>
- [60] Tsurudome Y, Hirano T, Kamiya H, Yamaguchi R, Asami S, Itoh H, Kasai H. 2-Hydroxyadenine, a mutagenic form of oxidative DNA damage, is not repaired by a glycosylase type mechanism in rat organs. *Mutat Res*. 1998; 408(2): 121-127. [https://doi.org/10.1016/s0921-8777\(98\)00025-1](https://doi.org/10.1016/s0921-8777(98)00025-1)

- [61] Ferraz BRL, Guimaraes T, Profeti D, Profeti LPR. Electrooxidation of sulfanilamide and its voltammetric determination in pharmaceutical formulation, human urine and serum on glassy carbon electrode. *J Pharm Anal.* 2018; 8(1): 55-59. <https://doi.org/10.1016/j.jpha.2017.10.004>
- [62] Vanoni CR, Winiarski JP, Nagurniak GR, Magosso HA, Jost CL. A novel electrochemical sensor based on silsesquioxane/Nickel (II) phthalocyanine for the determination of sulfanilamide in clinical and drug samples. *Electroanalysis.* 2019; 31(5): 867-875. <https://doi.org/10.1002/elan.201800832>
- [63] Sibirian R, Sihotang H, Raja SL, Supeno M, Simanjuntak C. New route to synthesize of graphene nano sheets. *Orient J Chem.* 2018;34(1): 182-187. <http://dx.doi.org/10.13005/ojc/340120>
- [64] Ng, L.L., Development and Validation of Analytical Procedures, Analytical Testing for the Pharmaceutical GMP Laboratory, 2022, pp. 143-167. <https://doi.org/10.1002/9781119680475.ch5>
- [65] Horwitz W, Albert R. The Horwitz ratio (HorRat): A useful index of method performance with respect to precision. *J AOAC Int.* 2006; 89(4): 1095-1109. <https://doi.org/10.1093/jaoac/89.4.1095>
- [66] Xiao J, Shi S, Yao L, Feng J, Zuo J, He Q. Fast and ultrasensitive electrochemical detection for antiviral drug tenofovir disoproxil fumarate in biological matrices. *Biosensors.* 2022; 12(12): 1123. <https://doi.org/10.3390/bios12121123>
- [67] Jain P, Jagtap S, Chauhan M, Motghare RV. Electro-catalytic behaviour of self-assembled Cu-chitosan/f-MWCNT on glassy carbon electrode for detection of erythromycin in various samples. *Sens Bio-Sens Res.* 2023; 41: 100568. <https://doi.org/10.1016/j.sbsr.2023.100568>